

# Co-optimizing the Smart Grid and Electric Public Transit Bus System

Mertcan Yetkin, Brandon R. Augustino, Alberto J. Lamadrid, Lawrence V. Snyder

May 2020

## Abstract

We consider electric public transportation buses in an urban area, which can provide ancillary services to the electric grid during times in which they are not serving any public transit demand. Our model considers a single social planner who decides the optimal charging/discharging times and locations for each transit bus. By doing so, the transit authority and the operator of the electricity system co-optimize the power system to minimize the total operational cost of the grid, while satisfying additional transportation constraints on buses. We propose a mixed-integer quadratic program (MIQP) that can be viewed as an extension of a deterministic multi-period optimal power flow (MPOPF) problem. We demonstrate the capabilities of the model and the benefit obtained via a coordinated strategy. We further extend the deterministic formulation into two additional two-stage stochastic MIQP formulations to co-optimize the system when a renewable generator is present within the power grid as extensions from an existing model in the literature. Each stochastic formulation provides a different set of recourse actions to manage the variable renewable energy uncertainty: ramping up/down of the conventional generators, or charging/discharging of the transit fleet. We compare the efficacies of these recourse actions to provide additional managerial insights. We test our models using a modified IEEE benchmark instance and verify our results with different sized power networks. This study is motivated by a project with a large transit authority in California.

## 1 Introduction

The electrification of transportation systems presents challenges associated with the joint operation of power and transit systems. A question of interest, is to determine how a fleet of electric buses can best be integrated into public transportation infrastructure. In particular, the task at hand is to determine where and when to charge and discharge the buses such that operating is not a detriment to the power system, but rather, offers flexibility to the grid depending on the transportation-operational requirements. By co-optimizing, we ensure that the additional demand imposed by the transit authority is satisfied while inducing minimal stress on the power system.

Our challenge is to consider aspects such as storage, renewable energy, and transportation networks simultaneously in conjunction with the optimal power flow (OPF) problem [3]. Specifically, our model considers the following aspects: an underlying multi-period optimal power flow (MPOPF) model, uncertain renewables, energy storage, vehicle-to-grid capabilities, and electrification of transit networks. We discuss the literature related to each of these aspects next.

A subset of the topics studied in this manuscript have been extensively addressed in the literature (see e.g., [1, 8]). Riffonneau et al. [22] present an optimal power management scheme for photovoltaic (PV) systems with storage units. In [16], Levron et al. consider a microgrid with storage capabilities and aim to optimize the power consumption by balancing the power generation of renewable generators. However, these and other related papers differ from ours, as we aim to incorporate each of these aspects in one formulation.

The optimal power flow (OPF) problem, first studied in [7], is an optimization problem that determines the optimal dispatch in a power network, in which one solves for a network operating point that satisfies power flow equations and physical constraints such as thermal limits and line capacities [9]. The multi-period optimal power flow problem (MPOPF) is a natural extension of the OPF problem, in which there are components involving multiple time periods such as storage units. In particular, storage units provide the

capability of storing energy for a period of time and releasing it in a later time period, which introduces a temporal dependency rather than the snapshot of the system studied in the original OPF formulation. There are several works associated with the operation of the power grid by use of MPOPF, alternatively known as dynamic power flow (DOPF). By utilizing an MPOPF formulation, one can provide additional services to the power grid, such as voltage stability regulation and ramping reserves, which, in general, are referred to as *ancillary services* in the power systems literature [24]. The role of ancillary services in MPOPF is studied by Yao et al. [28], who propose an MPOPF formulation that incorporates demand-responsive loads specifically to improve steady-state voltage stability. Similarly, Costa and Costa [10] present a DOPF-based model to clear both energy and spinning reserve day-ahead markets. In the present work, we extend the standard MPOPF formulation to incorporate a fleet of public transportation buses that have the capability to charge and discharge within the power network. Moreover, ancillary services are provided by uncertain renewable energy generation, which serves as ramping reserves [15].

Bukhsh et al. [5], propose a stochastic MPOPF model to cope with the uncertainty stemming from renewable generators. A sparse formulation of a robust MPOPF problem with storage units and renewable generators is provided by Jabr et al. [14]. In this work, they provide a solution methodology that utilizes receding horizon control. In [13], Chen et al. propose an MPOPF formulation that integrates wind farms into the generation portfolio. In [18], the authors address the non-convexity in the power flow equations and uncertainty in renewable generation in terms of both active and reactive power. Their model incorporates transmission constraints and reactive capability curves of both conventional and renewable generators. To incorporate uncertain generation in our work, we also propose two additional formulations extended from stochastic MPOPF.

From a power systems perspective, our work can be considered as an extension of the MPOPF problem with (*mobile*) storage units. Note that, the storage units are the buses in the transit fleet with additional operational constraints related to the transportation system. Many papers model the use of energy storage in the power grid. As a closely related work, a model similar to ours can be found in [32]. Here, the authors consider an MPOPF formulation that incorporates large-scale standalone battery energy storage devices to reduce the fluctuations in the grid and to handle peak shaving in the grid. The objective in the formulation is to minimize the total generation cost (which can be different in each time period) including the charging and discharging costs of the batteries. They also argue that the batteries may be used to handle the uncertainty introduced when renewable energy sources are considered. Note, however, that no public transportation aspects are considered in their work.

There are several works in the transportation literature investigating different problems associated with the electrification of the transportation systems. In [26], the authors propose a mathematical formulation to locate the charging stations within an urban transportation network. They further analyze the environmental outcomes, including emission of gases, based on a case study in the city of Stockholm. The authors of [27] extend the formulation proposed in [26] by incorporating additional constraints on the charging times of the transit buses and analyze the impacts using a similar case study in Stockholm. From a different perspective, the authors of [30] investigate the effect of ambient temperature in the energy consumption of autonomous electric vehicles. Their results are demonstrated with a data-driven simulated transportation network in New York City. Tangentially, Wei et al. [25] focus on the coordinated operation of transportation and power systems. They assume an electrified transportation network capable of wireless power transfer coupled with a power network. They propose an optimal traffic–power flow model optimizing the generation schedule and congestion tolls as a mixed-integer nonlinear program with traffic user equilibrium constraints.

The study of interdependent systems typically necessitates the use of multi-objective optimization techniques. In [2], the authors provide an overview of multi-objective planning of distributed energy resources (DERs) where the objective function involves terms from different perspectives including distributed energy resources developer, distribution system operator, and regulator. Specifically, they consider distributed generators (DGs) as the DER. In fact, they underline the importance of DER integration and argue that poor integration of DER can result in increases in losses and voltage and network instability. Besides, they point out the trade-off between formulation accuracy and optimization of the problem and suggest the use of realistic models combined with an accurate robust solution methodology. The insights provided in [2] exemplify the benefits obtained by a co-optimization framework. In our case, the co-optimization is considered between the independent system operator (ISO) of the power network and the transit authority.

From the perspective of interdependent systems, there are few works focused on the joint operation of

electric vehicles and the power grid. [31] address the problem of privately owned electric-vehicle charging coupled with the power network. Similarly, in [4], the authors aim to coordinate plug-in electric vehicles in a multi-objective security-constrained dynamic optimal power flow problem to minimize the total operation cost and emission. Tangentially related, [25] address the joint operation to optimize the traffic-power flow in an electrified network. In [31], the authors propose a multi-objective method for charging/discharging electric vehicles to minimize the total operational costs and emissions. Their optimization problem is formulated as a mixed-integer nonlinear program. An important assumption in their methodology is that the EV owner should decide the parking time for charging/discharging one day before. This assumption is one of the key differences between public and private means of transportation. In our model, by considering public transportation, we have complete control over the transit fleet, whereas, in the case of private transportation, the availability of electric vehicles is limited. Specifically, in our study, the decision of when and where to charge/discharge is made as a consequence of the joint operation between the independent system operator (ISO) and the public transportation authority (TA).

A related methodology to ours can be found in [17]. The authors study a planning problem that decides the locations and sizes of charging stations by considering a coupled transportation network and power network. Specifically, they seek to determine a long-term plan with a horizon of  $\approx 10$  years. An immediate drawback is that they assume that all information (electricity prices, infrastructure costs, demand, technology) will be relatively unchanged over their planning horizon of 10-30 years. Thus, having such a long term strategy may not be preferable. Further, the OPF problem is typically solved many times a day, sometimes as often as every five minutes [6], whereas their formulation couples the transportation aspects with OPF only once at a given stage of length 10 years, and the second is 30 years. From a formulation standpoint, a critical issue in [17] is how they incorporate EV charging demand into the OPF framework. More specifically, the authors calculate the power injection of each node after charging stations connect to the power grid. Their calculation leads to a mismatch of units being considered in the formulation. Precisely, the charging requires energy (power accumulated over time), whereas the OPF addresses the instantaneous power flow. Thus, one should carefully incorporate a time dimension in order to specifically account for this in the formulation. This illustrates one reason that MPOPF is typically utilized for incorporating storage units in the literature.

In sum, our work differs from the related works in the literature in the following aspects: we consider *(i)* a fleet of electric vehicles operated by a single authority, *(ii)* operational constraints related to the transit fleet while providing services to the power grid, *(iii)* schedules for the battery (transit bus) connection, and *(iv)* relocation of the batteries within the power grid.

To the best of our knowledge, we provided the first formulation to address this problem to the necessary level of detail in [29]. Further, we extend our preliminary work in [29] to address the joint operation of an electric public transit system and the power system, specifically when the fleet is “off-schedule.” We use “off-schedule” to refer to the set of time periods when the buses are not on their routes. Our primary contributions are as follows:

1. We provide a deterministic formulation that jointly optimizes the operation of a public transit authority and an ISO.
2. In the presence of renewable generation, we further extend this model to two two-stage stochastic programs (2SSPs) with different recourse actions, including additional charging/discharging of the transit fleet and ramping up/down the conventional generators.
3. We additionally provide managerial insights: first, by conducting a benefit analysis of coordinated optimization; and second, by demonstrating potential benefits of alternative recourse actions in the presence of variable renewable energy uncertainty.

The rest of the paper is organized as follows. In Section 2 we provide a formal definition of the problem. In Section 3 we introduce the deterministic formulation of the optimization problem. In Sections 4.1 and 4.2 the two 2SSP formulations are provided. Numerical results are provided in Section 5 and Section 6 concludes the paper. Additional content can be found in Appendices A, B, C, and D.

## 2 Problem statement

We consider a single social planner who manages both the power and public transit systems. The goal of the social planner is to co-optimize the joint operation of these two systems, by optimizing the charging/discharging of the transit bus batteries when buses are off-schedule, over a horizon of one day. The only operational requirement on the transit buses is that they have to be fully charged before starting their schedules on the following day. The following decisions are addressed in the formulation while satisfying operational constraints: *(i)* where, among a prespecified subset of nodes that serve as charging stations, to locate transit buses to charge/discharge, *(ii)* how much electricity to charge/discharge, and *(iii)* power dispatch.

We simplify the problem by assuming the following:

- All of the information related to the power network is known (topology, generator limits, line limits, etc.), except the ramping costs of conventional generators (which will be investigated in Section 5.4.2).
- Over the course of one day (the horizon) the topologies of both the transportation and power networks remain fixed. The power network is provided as a graph with lines as the power lines and nodes as the connection point of lines. In the transportation network, the nodes of the graph are interpreted as charging stations, and the lines as the transit routes among charging stations. Note that the charging stations in the transportation network act as coupling points between the two networks since they also appear as a subset of nodes in the power network.
- Electricity demand is known for the entire horizon, with the further assumption that an accurate day-ahead estimation of the demand is accessible.
- Direct current (DC) microgrids are in consideration as presented in [9]. This assumption is useful for simplifying the computational complexity of our optimization problem since the alternating current OPF problem is known to be nonlinear and non-convex [11].
- We assume black start capabilities for conventional generators. This assumption eliminates the start-up cost of conventional generators.
- All of the information related to transportation aspects are known (i.e. transportation network, schedules, travel times).
- All of the information related to batteries of the transit vehicles are known (the charge/discharge rate, total capacity, efficiency). The efficiency of the battery is same for charging and discharging. This assumption does not greatly affect the complexity of the formulation.
- Each charging/discharging station in the network has enough capacity for the entire fleet to charge simultaneously at one location. A related discussion is also provided in Appendix B.

## 3 Deterministic formulation

In this section, we present the deterministic formulation to co-optimize the operation of the transit fleet and the power grid. The formulation can be seen as an extension of the MPOPF problem with additional transportation aspects. The problem is a mixed-integer quadratic program (MIQP). The following components are captured by this formulation:

- Ensuring each bus has a full battery at the end of their off-schedule.
- Dispatch of power subject to physical constraints of the grid, such as ramping rates, transmission limits, etc.
- Charging/discharging of the buses subject to physical constraints with respect to the batteries of the transit buses, such as charging capacity, charging/discharging rate.

- Relocation of the buses subject to constraints related to the travel time of the buses depending on the node to connect to the electrical grid.

Due to space limitations, we provide the complete deterministic formulation in Appendix B, and we verbally describe the model in this section.

Our objective aims to minimize a convex combination, with coefficient  $\alpha$ , of the total power generation cost and the charging/discharging cost of the transit buses. As an overview, the model contains standard DC optimal power flow constraints with adjustments to include the effects of charging and discharging. Then, based on the fleet’s schedule, we ensure initial and final battery levels are respected. Also, the model includes updates for the battery levels. Based on assignment constraints, we ensure that a bus can either traverse the network or be stationed at a connection point for charging/discharging. Specifically, a bus can only relocate between two points in the power network if there is enough time available. We initially assign all of the fleet to a depot node. In addition, we have several bounds on ramping amounts of generators, generation amounts, line flows, charge/discharge amounts of batteries, and battery levels.

The two terms in the objective function each “belong” to a different party: The generation costs are incurred by the power grid operator while the charging costs are incurred by the transit operator. We use a convex combination of these two terms since they are usually in different scales, and since the central decision-maker may wish to place more or less weight on one term or the other. Similarly, in the stochastic models presented in the following sections, we use a convex combination of costs that are in different scales, in order to differentiate between the costs of different parties in this cooperation. In all of our numerical experiments, we set the convex combination coefficient,  $\alpha$ , to 0.5. Based on the requirements of the specific application, one can examine different objective terms such as line losses, voltage deviations, and many others tailored towards the desired goal. Note that, due to the specific application, we consider off-schedule periods as a single block of time (i.e. 5 pm - 4 am), and formulate this accordingly. Nonetheless, in the presence of multiple blocks, one should account for initial and final conditions on the battery levels for each block of off-schedule times.

## 4 Two-stage stochastic formulations

In this section, we consider renewable generation units (e.g., wind generators) within the power grid. In each time period, the quantity of renewable generation is random. We incorporate the uncertainty regarding the renewable generation units using scenarios in a two-stage stochastic modeling approach. Each of these scenarios represents one realization of wind generation distribution. The details of the scenario generation scheme are described in Section 5.2. In addition to the assumptions listed in Section 2, we assume that a forecast of the renewable generation is available over the course of one day, though the actual generation may differ randomly from the forecast.

Specifically, we present two different two-stage stochastic formulations, which assume different recourse actions. In the first formulation (Section 4.1), the recourse action is ramping up/down the conventional generators, whereas in the second formulation (in Section 4.2), the recourse is additional charging/discharging of the transit fleet. The first formulation assumes that the ISO is taking the recourse actions to mitigate the uncertainty, whereas the second assumes the transportation authority is doing so.

### 4.1 Ramping-based formulation

The following formulation can be considered as an extension of the two-stage stochastic single-period OPF formulation presented by Morales et al. [20] in the sense that we have the additional aspect of transportation and related operational constraints in the first stage. Briefly, we have the following set of decisions in addition to those listed in Section 3: a first-stage commitment of the renewable generation units on how much to generate; and a second-stage adjustment of power generation via ramping up/down the conventional generators. We again omit the complete model and provide the details in Appendix C.

Our objective is the summation of first-stage costs (as in the deterministic objective function) and second-stage costs including the expected renewable generation costs and expected ramping costs. Added to the constraints captured in the deterministic model in Section 3 are the second-stage nodal balance and flows. We are further constrained by limits on renewable generation, limits on second-stage ramping, and limits

on shedding in the second stage. Distinctively from the two-stage stochastic OPF formulation presented in [20], we have constraints on the transit bus battery levels, charging limits, and transportation constraints. More importantly, we have each of the OPF constraints repeated for multiple time periods rather than a single time period presented in [20], where the time periods are coupled via batteries on the transit fleet. The inclusion of multiple periods in the formulation increases the complexity of the problem dramatically.

## 4.2 Charging/discharging-based formulation

Rather than handling the uncertainty by ramping up/down the conventional generators, we now consider this service to be handled by the transportation authority via additional charging/discharging of the transit vehicles in the second stage. We assume that the realization of the scenarios occurs very close to real-time so that there is not enough time to relocate the transit buses after the scenario realizations. Then, we have the following set of decisions in addition to the ones in Section 3: a first-stage commitment of the renewable generation units on how much to generate; and an additional second-stage charging/discharging of transit fleet.

Before providing the complete formulation, a complete table of nomenclature can be found in Appendix A. Then, the formulation of the 2SSP whose recourse is charging/discharging of the transit buses is given as follows:

$$\begin{aligned} \min \quad & (1 - \alpha) \left[ \sum_{t \in \mathcal{T}} \sum_{i \in \mathcal{N}_g} c_{it}^g p_{it}^g + c_{it}^{\prime g} (p_{it}^g)^2 + \sum_{\omega \in \Omega} \pi_\omega \left( \sum_{t \in \mathcal{T}} \sum_{i \in \mathcal{N}_r} c_{it}^r p_{it\omega}^r + \sum_{t \in \mathcal{T}} \sum_{i \in \mathcal{N}} c_{it}^{\text{shed}} p_{it\omega}^{d,\text{shed}} \right) \right] \\ & + \alpha \left[ \sum_{t \in \mathcal{T}} \sum_{b \in \mathcal{B}} \sum_{i \in \mathcal{N}_b} c_{it} (p_{ibt}^c - p_{ibt}^{dc}) + \sum_{\omega \in \Omega} \pi_\omega \sum_{t \in \mathcal{T}} \sum_{b \in \mathcal{B}} \sum_{i \in \mathcal{N}_b} c_{it\omega}^+ (p_{ibt\omega}^{c,+} - p_{ibt\omega}^{dc,+}) \right] \end{aligned} \quad (1)$$

subject to:

$$p_{it}^g + p_{it}^r - \sum_{b \in \mathcal{B}} p_{ibt}^c + \sum_{b \in \mathcal{B}} p_{ibt}^{dc} - p_{it}^d = \sum_{j:(i,j) \in \mathcal{L}} p_{ijt} - \sum_{j:(j,i) \in \mathcal{L}} p_{jit} \quad \forall i \in \mathcal{N}, t \in \mathcal{T} \quad (2)$$

$$p_{it\omega}^r - p_{it}^r - \sum_{b \in \mathcal{B}} p_{ibt\omega}^{c,+} + \sum_{b \in \mathcal{B}} p_{ibt\omega}^{dc,+} + p_{it\omega}^{d,\text{shed}} = \sum_{j:(i,j) \in \mathcal{L}} (p_{ijt\omega} - p_{ijt}) - \sum_{j:(j,i) \in \mathcal{L}} (p_{jit\omega} - p_{jit}) \quad \forall i \in \mathcal{N}, t \in \mathcal{T}, \omega \in \Omega \quad (3)$$

$$p_{it}^g = 0 \quad \forall i \in \mathcal{N} \setminus \mathcal{N}_g, t \in \mathcal{T} \quad (4)$$

$$p_{it}^r = 0 \quad \forall i \in \mathcal{N} \setminus \mathcal{N}_r, t \in \mathcal{T} \quad (5)$$

$$p_{it\omega}^r = 0 \quad \forall i \in \mathcal{N} \setminus \mathcal{N}_r, t \in \mathcal{T}, \omega \in \Omega \quad (6)$$

$$-\bar{\theta} \leq \theta_{it} \leq \bar{\theta} \quad \forall i \in \mathcal{N}, t \in \mathcal{T} \quad (7)$$

$$-\bar{\theta} \leq \theta_{it\omega} \leq \bar{\theta} \quad \forall i \in \mathcal{N}, t \in \mathcal{T}, \omega \in \Omega \quad (8)$$

$$\theta_{1t} = 0 \quad \forall t \in \mathcal{T} \quad (9)$$

$$\theta_{1t\omega} = 0 \quad \forall t \in \mathcal{T}, \omega \in \Omega \quad (10)$$

$$p_{ijt} = \frac{\theta_{it} - \theta_{jt}}{x_{ij}} \quad \forall (i, j) \in \mathcal{L}, t \in \mathcal{T} \quad (11)$$

$$p_{ijt\omega} = \frac{\theta_{it\omega} - \theta_{jt\omega}}{x_{ij}} \quad \forall (i, j) \in \mathcal{L}, t \in \mathcal{T}, \omega \in \Omega \quad (12)$$

$$-\bar{S}_{ij} \leq p_{ijt} \leq \bar{S}_{ij} \quad \forall (i, j) \in \mathcal{L}, t \in \mathcal{T} \quad (13)$$

$$-\bar{S}_{ij} \leq p_{ijt\omega} \leq \bar{S}_{ij} \quad \forall (i, j) \in \mathcal{L}, t \in \mathcal{T}, \omega \in \Omega \quad (14)$$

$$0 \leq p_{it}^g \leq \bar{p}_{it}^g \quad \forall i \in \mathcal{N}_g, t \in \mathcal{T} \quad (15)$$

$$-p_{it}^{\delta g} \leq p_{i,t+1}^g - p_{it}^g \leq p_{it}^{\delta g} \quad \forall i \in \mathcal{N}_g, t \in \mathcal{T} \setminus \{T\} \quad (16)$$

$$0 \leq p_{it}^r \leq \bar{p}_{it}^r \quad \forall i \in \mathcal{N}_r, t \in \mathcal{T} \quad (17)$$

$$0 \leq p_{it\omega}^r \leq \tilde{p}_{it\omega}^r \quad \forall i \in \mathcal{N}_r, t \in \mathcal{T}, \omega \in \Omega \quad (18)$$

$$0 \leq p_{it\omega}^{d,\text{shed}} \leq p_{it}^d \quad \forall i \in \mathcal{N}, t \in \mathcal{T}, \omega \in \Omega \quad (19)$$

$$e_{bT_b^1\omega} = e_b^1 \quad \forall b \in \mathcal{B}, \omega \in \Omega \quad (20)$$

$$e_{bT_b^2\omega} + \eta_b \sum_{i \in \mathcal{N}_b} \left( p_{ibT_b^2}^c + p_{ibT_b^2}^{c,+} \right) \delta t - \frac{1}{\eta_b} \sum_{i \in \mathcal{N}_b} \left( p_{ibT_b^2}^{dc} + p_{ibT_b^2}^{dc,+} \right) \delta t - s_b y_{bT_b^2} = \bar{e}_b \quad \forall b \in \mathcal{B}, \omega \in \Omega \quad (21)$$

$$e_{b,t+1,\omega} = e_{bt\omega} + \eta_b \sum_{i \in \mathcal{N}_b} \left( p_{ibt}^c + p_{ibt}^{c,+} \right) \delta t - \frac{1}{\eta_b} \sum_{i \in \mathcal{N}_b} \left( p_{ibt}^{dc} + p_{ibt}^{dc,+} \right) \delta t - s_b y_{bt} \quad \forall b \in \mathcal{B}, t, t+1 \in \mathcal{T}_b, \omega \in \Omega \quad (22)$$

$$e_b \leq e_{bt\omega} \leq \bar{e}_b \quad \forall b \in \mathcal{B}, t \in \mathcal{T}_b, \omega \in \Omega \quad (23)$$

$$p_{ibt}^c + p_{ibt\omega}^{c,+} \leq \bar{p}_b^c z_{ibt} \quad \forall i \in \mathcal{N}_b, b \in \mathcal{B}, t \in \mathcal{T}, \omega \in \Omega \quad (24)$$

$$p_{ibt}^{dc} + p_{ibt\omega}^{dc,+} \leq \bar{p}_b^{dc} z_{ibt} \quad \forall i \in \mathcal{N}_b, b \in \mathcal{B}, t \in \mathcal{T}, \omega \in \Omega \quad (25)$$

$$p_{ibt}^c \geq 0, p_{ibt}^{dc} \geq 0 \quad \forall i \in \mathcal{N}_b, b \in \mathcal{B}, t \in \mathcal{T} \quad (26)$$

$$p_{ibt\omega}^{c,+} \geq 0, p_{ibt\omega}^{dc,+} \geq 0 \quad \forall i \in \mathcal{N}_b, b \in \mathcal{B}, t \in \mathcal{T}, \omega \in \Omega \quad (27)$$

$$p_{ibt}^c = 0, p_{ibt}^{dc} = 0 \quad \forall i \in \mathcal{N} \setminus \mathcal{N}_b, b \in \mathcal{B}, t \in \mathcal{T} \quad (28)$$

$$p_{ibt\omega}^{c,+} = 0, p_{ibt\omega}^{dc,+} = 0 \quad \forall i \in \mathcal{N} \setminus \mathcal{N}_b, b \in \mathcal{B}, t \in \mathcal{T}, \omega \in \Omega \quad (29)$$

$$\sum_{i \in \mathcal{N}_b} z_{ibt} + y_{bt} = 1 \quad \forall b \in \mathcal{B}, t \in \mathcal{T}_b \quad (30)$$

$$z_{ibt} + z_{jbt'} \leq 1 \quad \forall t' \in \mathcal{T}_b, t < t' \leq t + \Delta t(i, j), \quad \forall i, j \in \mathcal{N}_b, i \neq j, b \in \mathcal{B}, t \in \mathcal{T}_b \quad (31)$$

$$z_{dbT_b^1} = 1 \quad d = \mathcal{N}_b(1), \forall b \in \mathcal{B} \quad (32)$$

$$y_{bt} = 0 \quad \forall b \in \mathcal{B}, t \in \mathcal{T} \setminus \mathcal{T}_b \quad (33)$$

$$z_{ibt} = 0 \quad \forall i \in \mathcal{N}_b, b \in \mathcal{B}, t \in \mathcal{T} \setminus \mathcal{T}_b \quad (34)$$

$$y_{bt} \in \{0, 1\} \quad \forall b \in \mathcal{B}, t \in \mathcal{T} \quad (35)$$

$$z_{ibt} \in \{0, 1\} \quad \forall i \in \mathcal{N}_b, b \in \mathcal{B}, t \in \mathcal{T} \quad (36)$$

The objective function (1) accounts for the conventional generation cost in the first stage, expected renewable generation cost, charging/discharging cost of the fleet in the first stage and expected charging/discharging cost of the fleet in the second stage. We have already introduced the following sets of constraints in the deterministic formulation in Section 3: first-stage DC optimal power flow constraints (2), (4), (5), (7), (9), (11), (13); bounds on generation (15), ramping (16), and first-stage charging/discharging (26), (28); assignment constraints for vehicle to charging station connection and vehicle relocation (30)-(36).

Now, we additionally have second-stage nodal balance and flow constraints (3), (8), (10), (12), (14); limits on renewable generation (17), (18); and limits on shedding in the second stage (19). Unlike the formulation presented in Section 4.1, we are also charging/discharging in the second stage. Thus, the battery level variables for vehicles  $e_{bt\omega}$  are now second-stage variables over the set of scenarios  $\omega \in \Omega$ . Also, update constraints for battery levels are replicated for each scenario in (20)-(23). Moreover, we have modified bounds on the charging/discharging of the vehicles in (24), (25). Note that the positioning variables for the vehicles  $z_{ibt}, y_{bt}$  remain as first-stage variables, since we assume that there is insufficient time to adjust the location of the vehicles after the scenario realizations.

## 5 Numerical experiments

In this section, we first provide (in Section 5.1) results of the case study for the deterministic formulation, then (in Section 5.2) the results of the stochastic formulations. Based on the transportation-electrification

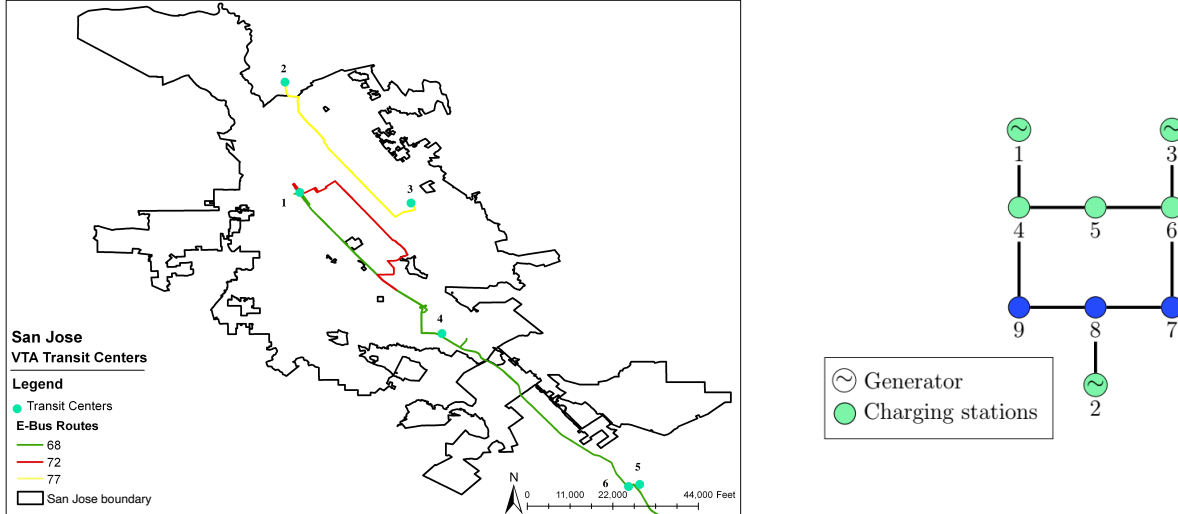


Figure 1: Transit layout (left) and power network schematic (right); charging stations are assumed to be located at Transit Centers

study on which we have collaborated with Santa Clara Valley Transportation Authority (VTA, <https://www.vta.org>), we will focus on a regional study around San Jose, CA. Our partner VTA has been undertaking the integration of electric transit buses into their fleet in the city of San Jose, initially for a selected number of routes within their operating region.

## 5.1 Case study for the deterministic formulation

We consider a case study consisting of synthetic but realistic data meant to reflect the actual transit network in San Jose, CA. We overlay the 9-bus power network from MATPOWER [33] atop the geographical area. Related parameters including demand ( $p_{it}^d$ ), line limits ( $\bar{S}_{ij}$ ), generation limits ( $\bar{p}_{it}^g$ ) and cost of generation ( $c_{it}^g, c_{it}^l$ ) are obtained from the MATPOWER case file. Figure 1 provides a visualization of the layout, indicating the locations of charging stations for electric bus connection in both the power and transit networks. Note that the transportation network is smaller than the power network since the charging stations are chosen to be a subset of nodes in the power network. In general, a power network is not confined within a city limit and hence is likely to encompass the transit region.

Line limits and demands from the 9-bus system are scaled down to the order of around 1 MWh so that we can clearly analyze the impact of the electric buses on the power network since battery energy capacities considered in this work are 0.66 MWh. Voltage angle limits  $\bar{\delta}$  are set to  $\pi/2$  and ramping limits are chosen to be  $\frac{\bar{p}_{it}^g}{5}$ . Since the standard case file in MATPOWER provides a snapshot of the system in one time period, we expand the demand profile over the multiple time periods based on information obtained from the California Independent System Operator (CAISO, <https://www.caiso.com>) for the San Jose region. Moreover, the charging/discharging costs ( $c_{it}$ ) in the objective function are the electricity prices obtained by averaging the prices as described in Section 5.4.1. The total daily demand and the price data are displayed in Figures 2 and 4, respectively. We also provide the expanded demand profile for the power network over multiple time periods in Figure 3.

We assume that the four transit buses are 40-foot Proterra Catalyst E2Max models; the data on battery consumption, battery capacity, and charge/discharge limits are obtained from Proterra (<https://www.proterra.com>). The battery efficiency is set to 0.9. We consider hourly time steps and a 24-hour horizon. The schedules of the buses and charging station locations are obtained from VTA, where  $\mathcal{T}_b$  represents the time periods in which the transit bus  $b$  is in its off-schedule.  $\Delta t(i, j)$  values are travel times between charging stations calculated using Google Maps (and discretized based on the resolution of the formulation). Thus, considering travel times as constants is a reasonable way to account for off-schedule times overlapping  $\approx$ non-working hours.

We performed the optimization using Gurobi version 8.1.0 [12], with the default settings. The hardware

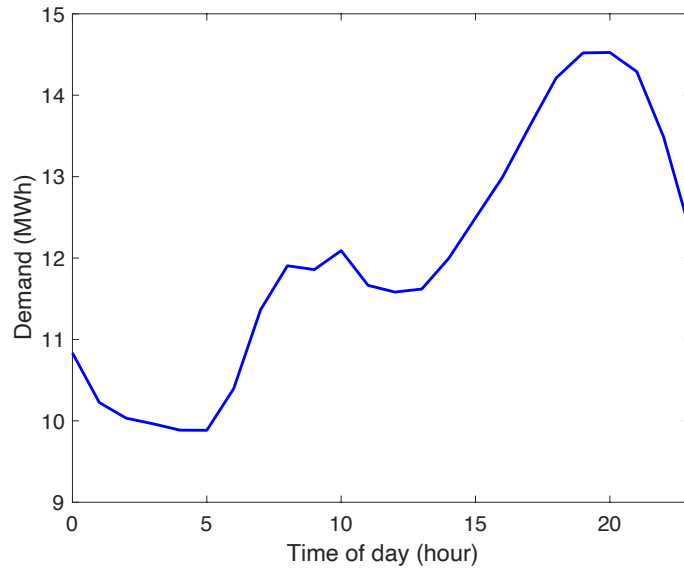


Figure 2: Daily demand data

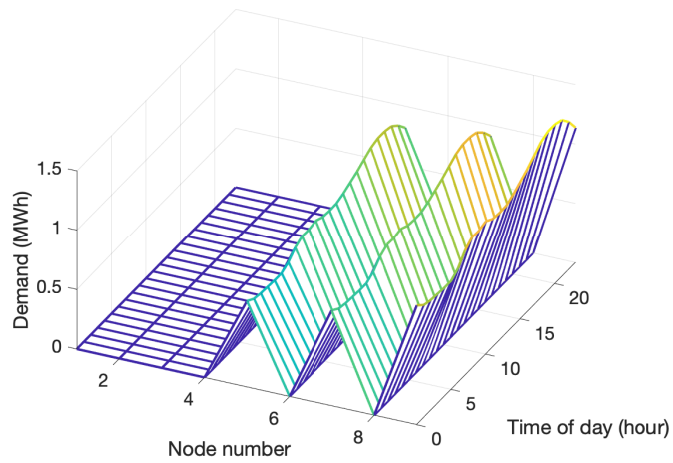


Figure 3: Complete demand profile in power network (constructed)

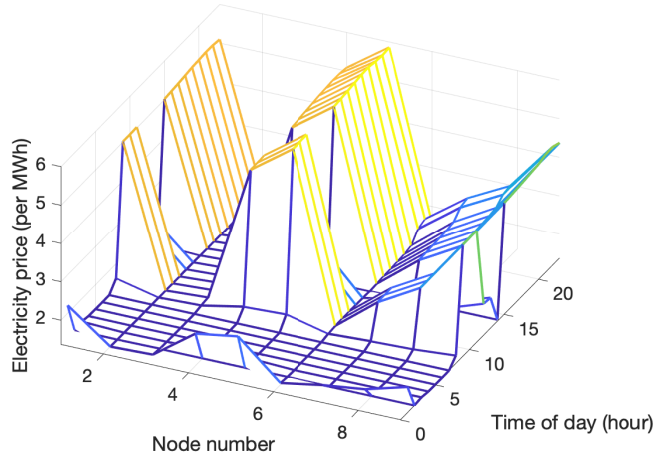


Figure 4: Price data

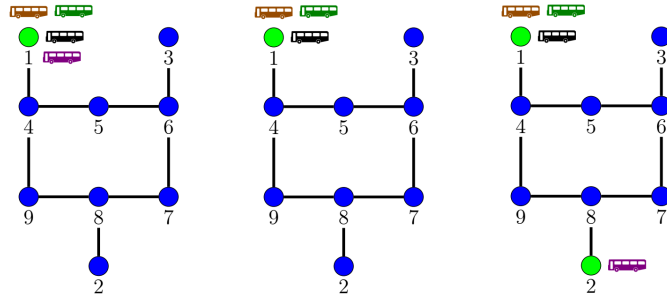


Figure 5: Transit bus locations for  $t = 21$ ,  $t = 22$  and  $t = 23$  in optimal solution

was 2.2 GHz Dual-Core Intel Core i7 and 8GB memory. The solution time for this model was approximately 23 seconds.

Figure 5 displays the optimal locations of the transit buses for 3 consecutive time periods. At the time  $t = 21$ , all of the four vehicles are located at node 1, the transit depot. In the next time period, three of the buses remain at node 1, while the fourth is in transit. At  $t = 23$ , this bus will arrive at its new location, node 2, in order to help decrease total generation cost. Figure 6a shows the generation and battery level profiles. In the optimal solution, battery levels in the first periods increase due to the operational constraints and decrease in the last periods since the price of electricity and the demand are high. Further, during the periods in which the transit buses are on their schedule, we can observe that the battery levels (i.e., the amount of energy stored in the batteries of the transit vehicles when they are not connected to the grid) are displayed as zero.

Figure 6b shows that the total operational cost and generation costs first slightly decrease then increase when we increase the battery capacity on the transit buses. This suggests that the presence of the batteries can alleviate some strain on the system even though the total generation amount increases. Moreover, we can observe that the charging/discharging cost is mostly negative and decreasing up to a certain level. Despite the fact that operational constraints on the transit fleet require more energy to be stored, the price difference over the course of the day causes the transit authority to be able to arbitrage and gain some profit. In Figure 7, we show that the generation profile changes dramatically as the battery capacities increase. Depending on the transit schedule, large batteries can cause added strain on the power system, while acting as generators during other periods.

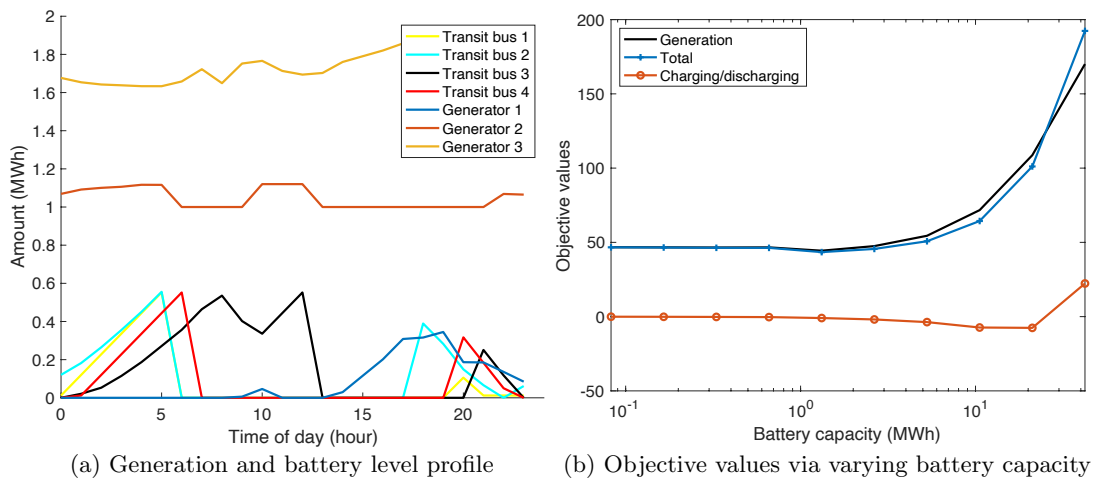


Figure 6: Optimization results

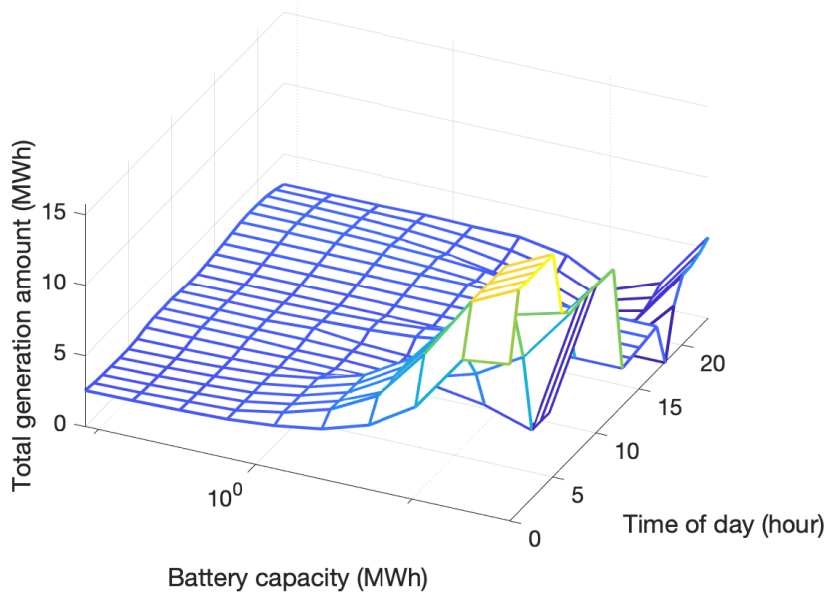


Figure 7: Total generation via varying battery capacity

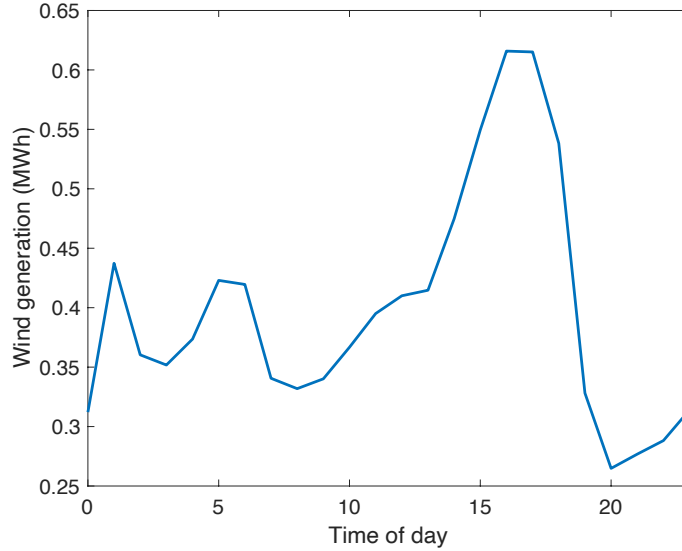


Figure 8: Daily wind generation amount for 09/09/19 in San Jose (simulated)

## 5.2 Case study for stochastic formulations

In this section, we consider the same instance described in Section 5.1, modifying the 9-bus system to include a wind generation unit located at node 4 in the power network displayed in Figure 5. No other changes are made to the 9-bus system. The generation cost of wind is assumed to be the minimum over the linear cost coefficients of conventional generation, that is,

$$c_{it}^r = \min_{i \in \mathcal{N}_g} \{c_{it}^g\}.$$

In this manner, we ensure that the wind generator is always the cheapest among all generators, conventional or renewable. The wind generation data is obtained from a simulation API (see [21, 23] for more details) for the day 09/09/19 within close proximity of the San Jose region with maximum generation capacity set at 1 MWh. That is, the data is synthetic, but closely approximates the true wind generation of the area under consideration. Figure 8 provides an illustration of the daily data. Moreover, we add normally distributed noise with mean zero and a small variance (in the order of  $\approx 0.01 MWh$ ) to create the desired number of scenarios. When one hundred scenarios are considered, we obtain the distribution shown in Figure 9.

The generated wind data is used as the renewable generation amount for each scenario in both of the 2SSP formulations. The charging/discharging prices in 2SSP formulations are derived as described in Section 5.4.2, and a visualization is provided in Figure 16. In each of the following sections, we are limited to only 10 scenarios for the renewable generation due to computational limitations. Note that the primary goal of these two models is to assess the capabilities of two different formulations in terms of wind utilization, since in reality, the renewable generation cost should be the smallest among all other costs, including the ramping cost of conventional generators. Hence, one should try to utilize wind generation as much as possible.

There is evidence of asymmetry in the ramping up and down of thermal generators. There are three identified sources for these costs: (1) *creep*, when components operate above the design temperature; (2) *thermal fatigue*, when changes in temperature result in mechanical failure; (3) *creep-fatigue* interactions, when the two effects above compound. In the ramp-up of thermal generators, these three effects are present, whereas in ramp-down the main effect is thermal fatigue [19]. For this reason, in the following numerical results, we use ramping costs defined by:

$$\begin{aligned} c_{it}^{g,+} &= 1.2c_{it}^g \\ c_{it}^{g,-} &= 0.5c_{it}^g. \end{aligned}$$

That is, for ramping costs we only consider the linear generation cost coefficient  $c_{it}^g$  to make ramping slightly cheaper than generation, and, ramping down is much cheaper than ramping up.

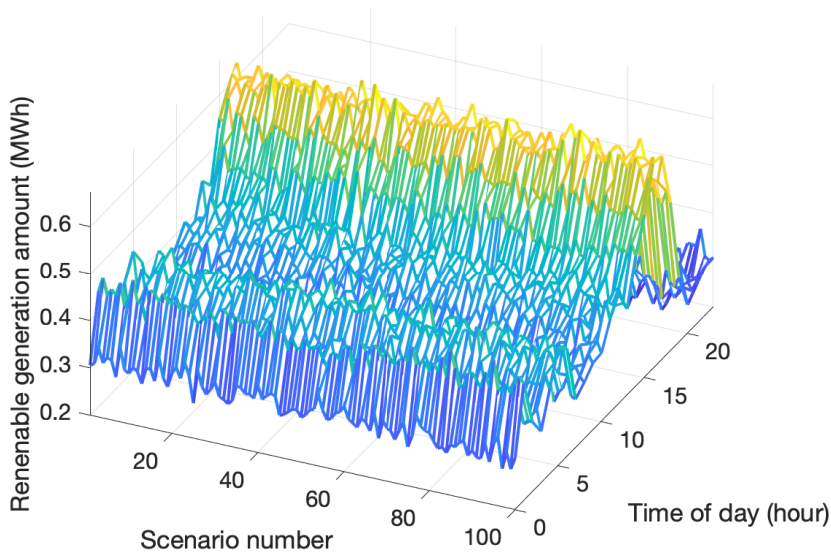


Figure 9: Wind generation distribution over scenarios

### 5.2.1 Case study for ramping-based formulation

Figure 10 gives a summary of the optimal solution of the formulation presented in Section 4.1. We observe that only one generator uses ramp-up in the second stage. Note that the behavior of the battery levels are similar to those resulting from the solution to the deterministic formulation in that they have a similar charging pattern; they charge in the early hours of the morning, as well as late at night. That is, regardless of whether or not the decision is being made by the social planner, the risk associated with deciding when to charge/discharge does not drastically affect the charging/discharging times of the transit buses. This could be attributed to the fact that the generators are flexible enough to handle fluctuations in the amount of renewable generation.

In Figure 11, we present the optimal values of wind generation corresponding to the second stage resulting from solving the optimization problem found in Section 4.1 across all time periods and scenarios. For each scenario, we find that wind-generated energy is utilized in its entirety. We calculate the wind utilization measure as follows:

$$\text{Wind Utilization} = \frac{\text{total wind usage in optimal solution}}{\text{aggregation of wind generation from scenarios}}. \quad (37)$$

In essence, wind utilization calculates the ratio of utilized wind generation (in the optimal solution) to the total available wind generation over all of the scenarios. Since we consider all of the scenarios in the calculation of the measure, it can be thought of as an average utilization over the scenarios. This is useful to quantify in general, since we would like to utilize as much wind energy as possible in the solution.

In our numerical results corresponding to the optimization problem found in Section 4.1, the wind utilization is found to be 1.0 (i.e., 100%). As such, in this case, ramping as a recourse action is flexible enough to handle the deviations in wind generation over the entire planning horizon. However, if we restrict the ramping quantity in the second stage to only allow for very small deviations in the generation, this total utilization might not be attainable. This is because the wind generator is limited to a total hourly (periodic) generation capacity of 1 MWh, whereas in our numerical experiments we allow for ramping that can introduce fluctuations on the order of  $\sim 100$  MWh.

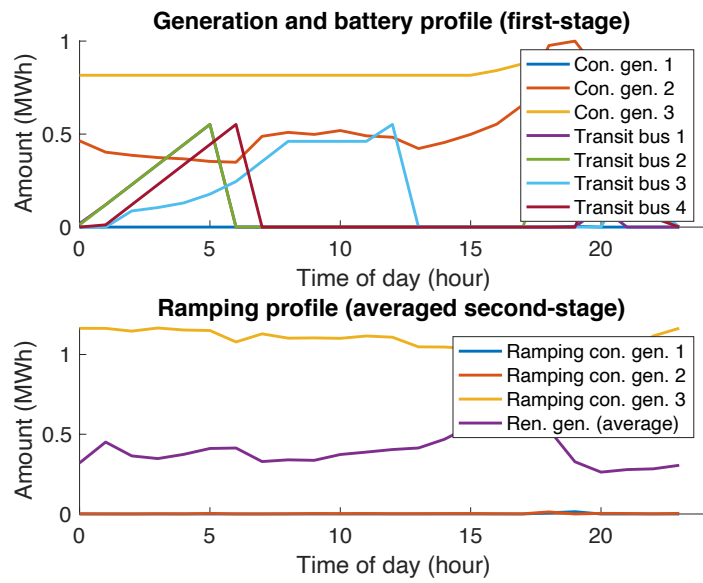


Figure 10: Optimum generation, charging, and ramping levels

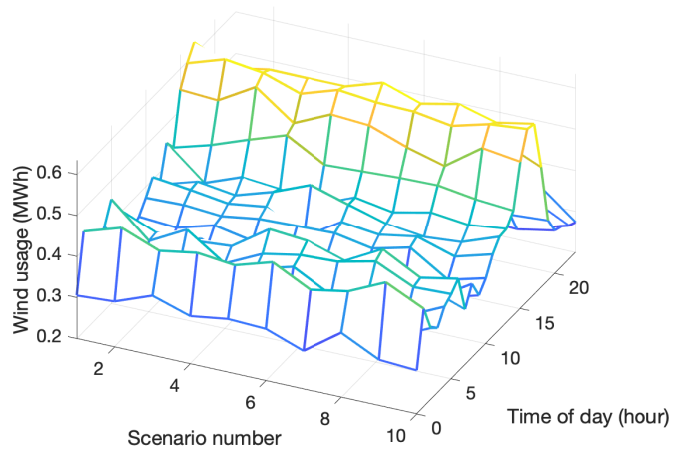


Figure 11: Wind usage amount in the optimal solution

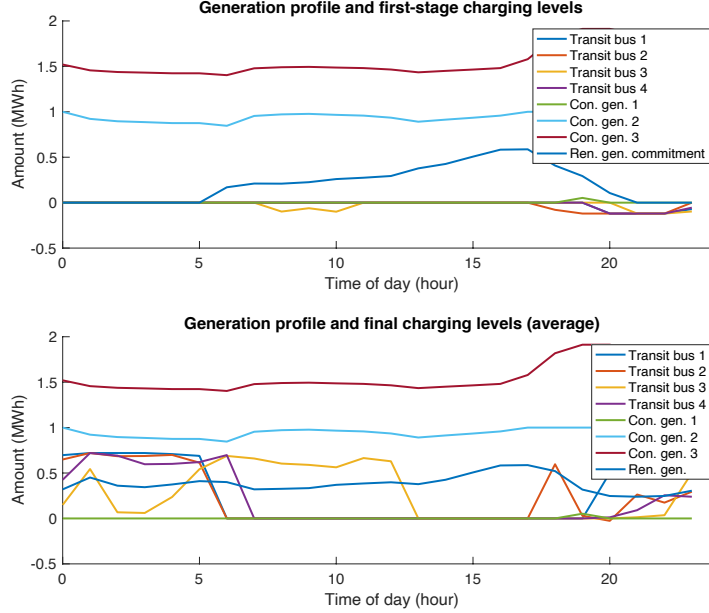


Figure 12: Optimum generation and charging levels

### 5.2.2 Case study for charging/discharging-based formulation

In Figure 12, we provide a summary of the solution of the formulation described in Section 4.2. It is clear that the generator outputs are much higher in the first stage compared to the solution of the alternative model displayed in Figure 10, as second-stage adjustment via ramping is not allowed in this formulation. Moreover, we also observe that the transit charging/discharging levels change in the second stage rather than in the first stage, to utilize the wind energy as much as possible.

Additionally, in Figure 13 one can view the battery levels of transit vehicles for each scenario (for 10 scenarios, as mentioned above). We can observe that the entire fleet adjusts its battery levels based on the availability of renewable generation while ensuring that the operational constraints are feasible. In particular, these operational constraints limit the solution space and make the recourse actions much more difficult than those of simple batteries.

Similar to the previous subsection, we calculate the wind utilization measure given by equation (37), and find that for the solution to the optimization problem given in Section 4.2 the total wind utilization is 0.9645 (96.45%). In Figure 14, we present the optimal values of wind generation corresponding to the second stage resulting from solving the the optimization problem found in Section 4.2 across all time periods and scenarios. One observation is that in this case, the solution is limited by operational constraints and battery capacities. As a result, compared to the previous utilization displayed in Figure 11, we find that the model from Section 4.2 does not fully utilize wind generation later in the day (roughly from  $t = 15$  and on). These underutilized time periods occur specifically when the fleet is serving public transit demand. However, if the fleet contains numerous transit buses with complementary off-schedules that span an entire day, the utilization would certainly be superior.

## 5.3 Larger power grids

To verify the capabilities of the proposed formulation for cooperation, we further test it when larger power networks are coupled with the transit network. In particular, from the MATPOWER [33] case files, we consider “case14”, “case30”, “case39”, “case57”, and “case118,” where the number denotes the number of nodes in the system. These cases are directly accessible within the MATPOWER instance list. We only modify these instances by scaling down the demand, which is done similarly to the procedure explained in Section 5.1. Note that the information associated with the transit fleet remains the same. We always assume the charging stations are connected at the first six nodes of the power system.

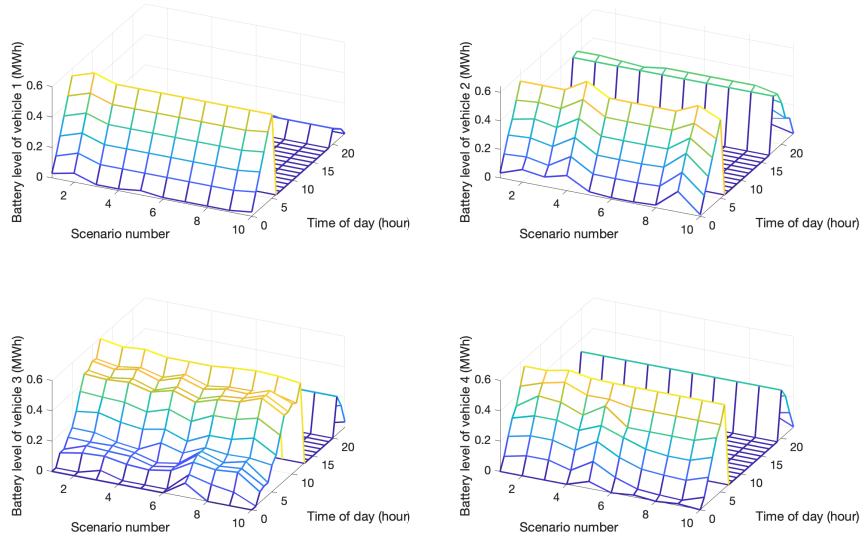


Figure 13: Battery levels of vehicles

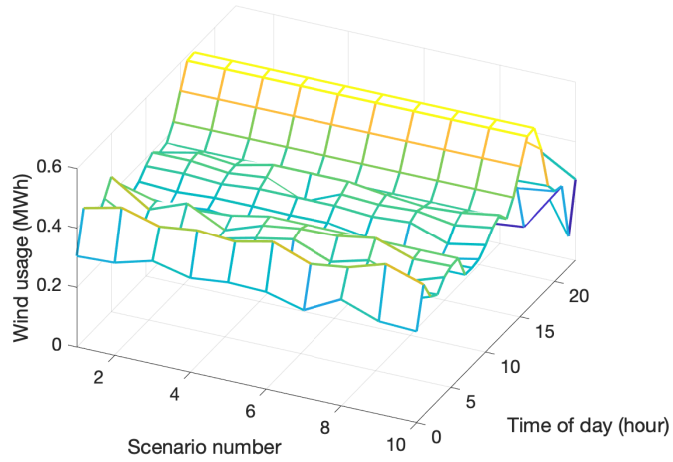


Figure 14: Wind usage amount in the optimal solution

System size	Solution time (s)
9 nodes	23.1256
14 nodes	0.3720
30 nodes	0.4434
39 nodes	0.4810
57 nodes	0.4285
118 nodes	1.1776

Table 1: Solution times of the deterministic formulation

Power grid case	Solution time (s)	Wind utilization
9 nodes	0.8120	1
14 nodes	2.3466	1
30 nodes	4.9761	1
39 nodes	6.8127	1
57 nodes	9.4370	1
118 nodes	146.8926	1

Table 2: Summary of results for the stochastic formulation with recourse action as ramping

We obtain similar findings in these instances. While imposing additional demand on the power network, the transit fleet can act as batteries for periods of time and alleviate generation costs by smoothing the generation profile. Moreover, in instances in which congestion is present, we observe the effect of the transit fleet more clearly, since the unit prices of electricity set by the optimal dual variables associated with the nodal balance equations can dramatically change over time (due to congestion), and the transit fleet could utilize an arbitrage strategy, which, in fact, benefits the whole system in cooperation.

Table 1 provides a summary of solution times for the deterministic formulation.

It is immediate to observe that the solution time of the deterministic formulation with our modified case9 instance is much higher than the rest of the cases. This is primarily related to the additional congestion introduced into the power network. Aside from the case9 outlier, we observe the solution times increase when we incorporate larger power networks.

Table 2 provides a summary of results for the ramping-based stochastic formulation on larger power networks. From the table, one can observe that we have complete wind utilization in every case, because ramping limits of conventional generators are large enough to compensate the uncertainty in the second stage. Moreover, in general, solution times increase when we integrate a larger power network into the formulation.

Finally, Table 3 provides a summary of results for the charging/discharging-based stochastic formulation on larger power networks. We can observe that in all of the cases, we have the same wind utilization (0.9645), since the charging limit of the transit fleet remains same in all of the formulations, and the fleet can compensate a portion of the uncertainty in the second stage. More importantly, we also observe that allowing second-stage charging/discharging of the fleet introduces additional complexity to the formulation, since solution times are much larger than those in Table 2.

## 5.4 Managerial insights

### 5.4.1 Benefit of coordinated optimization

In this section, considering the deterministic formulation, we evaluate the benefit of employing a coordinated strategy between the ISO and the transportation authority. To serve as a baseline, we consider their uncoordinated operation where both parties act to manage their own objectives. The uncoordinated optimization procedure is summarized in Algorithm 1.

Power grid case	Solution time (s)	Wind utilization
9 nodes	121.3390	0.9645
14 nodes	1690.1862	0.9645
30 nodes	32.7924	0.9645
39 nodes	47.3546	0.9645
57 nodes	52.4875	0.9645
118 nodes	991.3013	0.9645

Table 3: Summary of results for the stochastic formulation with recourse action as charging/discharging

---

**Algorithm 1** Uncoordinated optimization scheme

---

- 1: Feasible charging scenarios generated by ISO
  - 2: **for** each scenario **do**
  - 3:   ISO solves dispatch problem with additional demand determined by the scenario and obtains a set of prices from dual variables associated with nodal balance constraints
  - 4:   Using the prices, transit authority optimizes its own problem and obtains a charging/discharging policy
  - 5:   Charging/discharging policy is realized by ISO, and ISO objective value is obtained
  - 6:   Charging/discharging policy is evaluated under baseline prices to obtain transit objective
  - 7:   Total uncoordinated cost is calculated
  - 8: **end for**
- 

Step 1 of Algorithm 1 generates a given number of scenarios, which only factors feasible charging of batteries into consideration. That is, the charging anticipated by the ISO is guaranteed to satisfy transit-operational constraints. This proves to be beneficial to the ISO, as this procedure can be seen as educated anticipation from the ISO, where they have access to some information related to the transportation system. Step 3 simply solves an MPOPF without any of the transportation aspects in the formulation described in Section 3. In Step 4, only the transportation aspects such as charging/discharging and location/relocation of the transit buses are considered in a separate formulation. Then, Step 5 solves the formulation in Step 3 with the optimal charging/discharging obtained in Step 4 as an additional demand. Next, in order to make the comparison fair, in Step 7, we consider a set of baseline prices to evaluate the solution obtained in Step 4. This can also be seen as the average prices over the scenarios anticipated by the ISO.

For the coordinated optimization, the deterministic formulation in Section 3 is solved, with baseline prices and the objective value being calculated with convex combination coefficient  $\alpha = 0.5$  in the objective function (38). Now, since the uncoordinated cost accounts for the summation of the two costs (rather than a convex combination), we scale down the total uncoordinated cost by halving it, in order to make the comparison fair.

Figure 15 details the uncoordinated objective values for the transit authority, ISO, and their sum (all of the quantities are scaled down by 0.5 due to the presence of  $\alpha$  in the co-optimization), and compares these with the coordinated objective values. It is immediate to see that the total and ISO objective values are always worse in the non-cooperative case. An immediate reason is that the anticipation of charging schedules made by the ISO are quite different from the actual strategy employed by the transportation authority, and the power system incurs additional generation cost. However, since we consider charging prices that are averaged over scenarios as the baseline prices, the transit objective values are competitive between the two strategies. These results suggest that the ISO benefits largely from cooperation with the transit authority. This was expected since the ISO minimizes its cost when it has full knowledge of the optimal charging schedule, and anticipation of any deviation from the optimal charging schedule will of course worsen the ISO's operation.

We also tested the benefit of coordination in the larger power networks discussed in Section 5.3. Table 4 summarizes the results. Note that the non-cooperative objectives are calculated by taking the average of the objectives over 100 different anticipation scenarios. As expected, on average, the transit objectives in

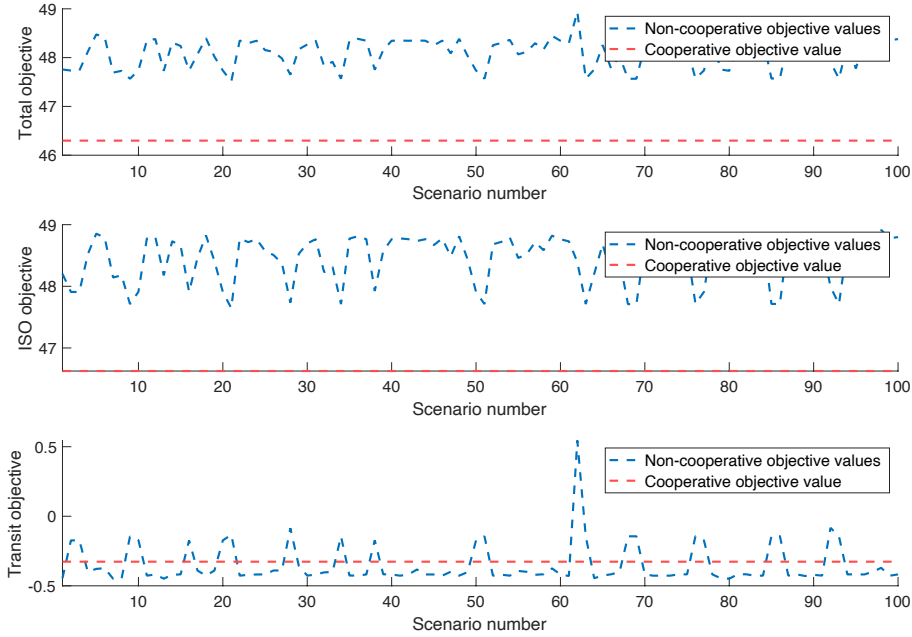


Figure 15: Comparison of objective values

Case	Coop. t. <sup>a</sup> obj.	Non-coop. t. <sup>a</sup> obj.	Coop. I. <sup>b</sup> obj.	Non-coop. I. <sup>b</sup> obj.
14 nodes	17.7027	17.7028	752.0961	752.0983
30 nodes	1.5947	1.5950	126.2755	127.8705
39 nodes	0.2724	0.2724	23.5928	23.5929
57 nodes	17.5882	17.5882	900.5379	900.5385
118 nodes	17.5838	17.5838	4092.912	4092.915
145 nodes	17.5269	17.5269	1320.0214	1320.0215

<sup>a</sup> Transit authority, <sup>b</sup> ISO

Table 4: Benefit analysis of the deterministic formulation (summary)

both strategies match, since we use the average prices (over 100 anticipation scenarios) as our electricity prices in the evaluation step. Moreover, we observe that in all of the cases the ISO benefits from the cooperative strategy, with the magnitude of the benefit becoming less significant when larger power networks are considered. This supports our previous results concluding that the scale of the battery capacities (or the transit fleet) plays a crucial role in the benefit obtained by a cooperative strategy. Observing the intricacies of the benefit analysis on stochastic formulations is yet another exploration. However, for the sake of conciseness, we believe that the primary aspect of the coordination is demonstrated.

#### 5.4.2 Potential benefits of alternative recourse actions

In this section, we are interested in the comparison of the two stochastic formulations presented in Sections 4.1 and 4.2. Recall that the first model investigates recourse actions taken by the ISO (ramping), whereas the second model considers the actions taken by the transit operator (using batteries to handle the fluctuations in the second stage).

Now, to ensure a fair comparison, we consider the same set of charging/discharging prices in both of the formulations. Note that in the second formulation, there are two sets of prices, corresponding to the prices in the first stage,  $c_{it}$ , and in the second stage,  $c_{it\omega}^+$ . These prices are obtained by solving the two-stage

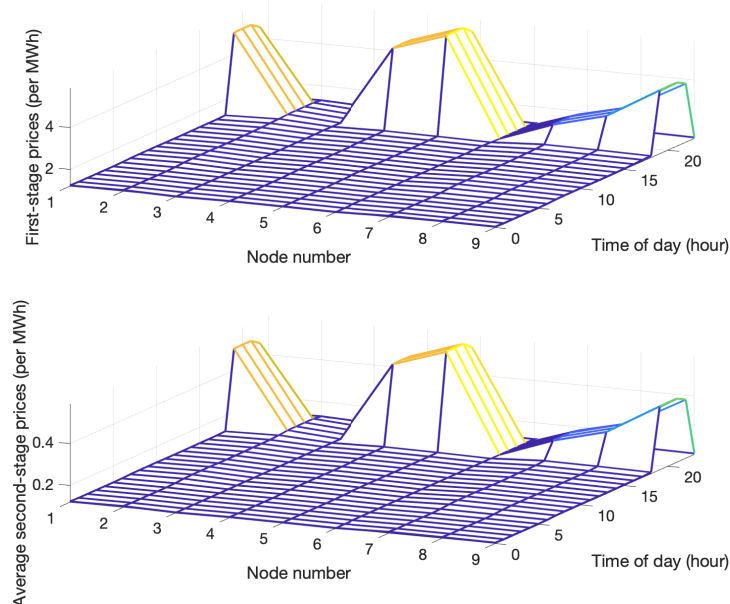


Figure 16: First-stage and second-stage prices for charging/discharging of the transit fleet

stochastic multi-period dispatch problem given in Appendix D. In more detail, the optimal values for the dual variables associated with the first-stage nodal balance equations determine the first-stage prices, and the second-stage prices are derived similarly. Figure 16 illustrates the first-stage prices and the average second-stage prices for charging/discharging of the transit fleet.

In both stages, we observe that prices sharply increase near the end of the day due to the extra stress imposed by the extra wind generation around similar times as previously shown in Figure 8. Moreover, the second-stage prices are much lower than the first-stage prices. This could be attributed to the fact that the second-stage flows are much smaller, as the scale of recourse actions is typically much smaller than that of the first-stage decisions.

Next, we analyze the costs in each of the two models provided in Sections 4.1 and 4.2. The following parameters are relevant:

- First-stage and second-stage charging/discharging prices  $(c_{it}, c_{itw}^+)$
- Renewable generation cost  $(c_{it}^r)$
- Ramp-up/down costs for conventional generators  $(c_{it}^{g,+}, c_{it}^{g,-})$

Observe that the renewable generation term appears in both of the objectives (62) and (1). Then, the only freedom we have is in determining ramping costs for conventional generators. Based on this, we vary the ramping cost values and obtain a trade-off between the costs of the two models. We provide the scheme for comparing the two stochastic formulations in Algorithm 2.

---

**Algorithm 2** Efficacy analysis for the stochastic formulations

---

- 1: **for** each ramp-up/down cost **do**
  - 2:   Using ramping costs, solve the two-stage stochastic MPOPF to obtain first-stage and second-stage charging/discharging prices
  - 3:   Using the first-stage prices and ramping costs, solve the model with ramping as the recourse action and obtain an objective value
  - 4:   Using the first-stage and second-stage prices, solve the model with charging/discharging as the recourse action and obtain an objective value
  - 5: **end for**
-

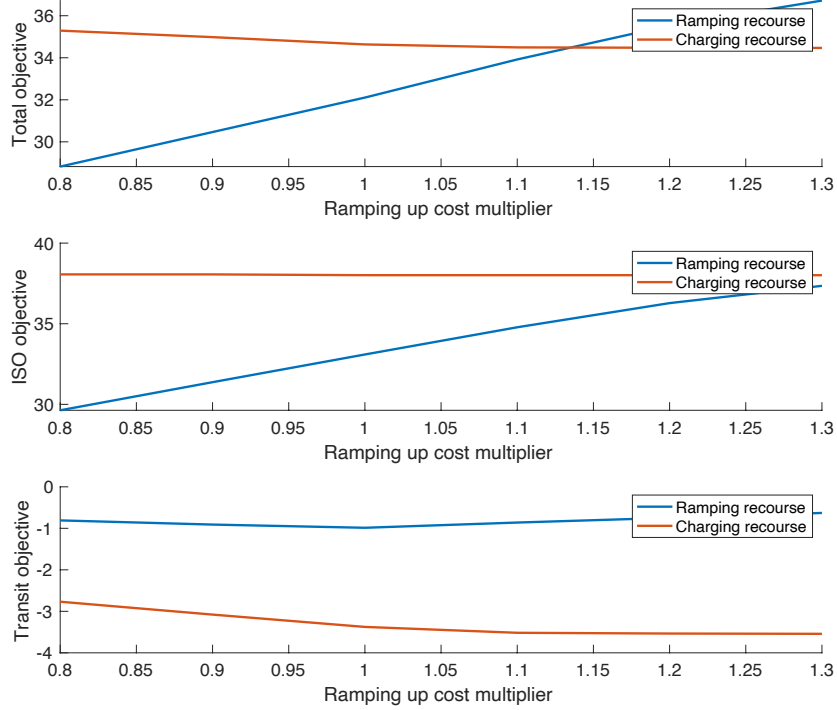


Figure 17: Comparison of objectives in stochastic formulations by varying ramp-up cost

In Algorithm 2, we provide the procedure to obtain the trade-off by calibrating the ramping costs in objective (62). In more detail, we systematically vary the ramping costs and obtain the adjusted prices for both first and second stages via locational marginal prices in step 2. Currently, for simplicity, in step 2, we do not consider the added demand by the transit fleet. Alternatively, one could also incorporate an average demand of transit charging/discharging. Then, by way of these new prices, we separately solve the two formulations and compare their objective values. Note that, in our experiments, we only vary the ramp-up cost by changing the multiplier  $\gamma$  in the following manner:

$$\begin{aligned} c_{it}^{g,+} &= \gamma c_{it}^g \\ c_{it}^{g,-} &= 0.5c_{it}^g, \end{aligned}$$

where  $\gamma \in \{0.8, 0.9, 1, 1.1, 1.2, 1.3\}$ . By allowing the value of  $\gamma$  to vary over these values, we obtain the results in Figure 17.

As can be seen, when the ramp-up cost multiplier value is around 1, the total objective values in the two models become competitive. Since having the value around 1 is reasonable, we can conclude that the recourse action provided by charging, as opposed to ramping, can be a useful alternative depending on the generator ramping costs. Moreover, it is interesting to observe that the transit objective in the second formulation is much smaller. One possible reason for this could be that the batteries have more flexibility in the second formulation since they can also arbitrage between the first and second stages, whereas in the first formulation, they can only charge/discharge in the first stage.

We further conducted a similar analysis when larger power networks are coupled with the transit network. In general, we obtained similar findings in which the trade-off values for  $\gamma$  were close to 1. This supports the idea that the two 2SSP models can be alternatives to each other depending on ramping costs, and more importantly, total battery capacity. We omit further details to avoid displaying repetitive findings.

In a broad view, in this section, we compared two types of recourse actions in our framework. It is crucial to note that for additional flexibility promoting the integration of renewable generators, one can utilize these two recourse actions simultaneously.

## 6 Conclusion

In this work, we propose a deterministic mathematical programming formulation to co-optimize the operation of the public transit system and the power grid when the transit buses are in their off-schedule considering generators without uncertainty. Furthermore, we propose two different two-stage stochastic programming formulations, in which uncertainty is present within the generation units with different recourse actions: (i) ramping up/down the conventional generators, (ii) additional charging/discharging of the transit fleet.

Our numerical results demonstrate that coordinated operation between the ISO and transit authority can decrease the generation costs while ensuring that the charging can be done at no detriment to the power system. Additionally, we conclude that in the presence of renewable generators, charging/discharging of the fleet as a recourse action can serve as a useful alternative to ramping up/down the conventional generators. Yet, as detailed, the benefits of charging/discharging of the fleet as a recourse action depend on battery capacities, ramping costs, and ramping limits. Our proposed formulations are general in the sense that they can incorporate different schedules, and different renewable generation units, different transportation and power networks.

A valuable extension to these formulations would be to consider separate renewable generation units owned and managed by the transportation authority. In this case, the charging/discharging costs of the vehicles would depend on which generator is chosen to be used. That is, it would be the same as the generation cost if they use their own generators, and it would be the market price derived from locational marginal prices if they use other generators within the power grid operated by the ISO.

Moreover, due to the fine resolution of the formulation, incorporating a physical model for battery degradation within the framework would decrease the losses further, and increase the flexibility of the co-optimization overall. Within the capabilities of the current framework, external effects such as battery degradation and charging technology could be represented by updating the necessary parameters. Finally, it is worth noting that while our approach does not address the decision of locating charging stations, the solutions obtained from our model would provide valuable managerial insights about the charging station locations.

## References

- [1] A. Agrawal, M. Kumar, D. K. Prajapati, M. Singh, and P. Kumar. Smart public transit system using an energy storage system and its coordination with a distribution grid. *IEEE Transactions on Intelligent Transportation Systems*, 15(4):1622–1632, 2014.
- [2] A. Alarcon-Rodriguez, G. Ault, and S. Galloway. Multi-objective planning of distributed energy resources: A review of the state-of-the-art. *Renewable and Sustainable Energy Reviews*, 14(5):1353 – 1366, 2010.
- [3] O. Alsac and B. Stott. Optimal load flow with steady-state security. *IEEE Transactions on Power Apparatus and Systems*, PAS-93(3):745–751, 1974.
- [4] R. Azizipanah-Abarghooee, V. Terzija, F. Golestaneh, and A. Roosta. Multiobjective dynamic optimal power flow considering fuzzy-based smart utilization of mobile electric vehicles. *IEEE Transactions on Industrial Informatics*, 12(2):503–514, April 2016.
- [5] W. A. Bukhsh, C. Zhang, and P. Pinson. An integrated multiperiod opf model with demand response and renewable generation uncertainty. *IEEE Transactions on Smart Grid*, 7(3):1495–1503, May 2016.
- [6] M. B. Cain, R. P. O’neill, A. Castillo, et al. History of optimal power flow and formulations. *Federal Energy Regulatory Commission*, 1:1–36, 2012.
- [7] J. Carpentier. Contribution a l’etude du dispatching economique. *Bulletin de la Societe Francaise des Electriciens*, 3(1):431–447, 1962.
- [8] T. Chen, B. Zhang, H. Pourbabak, A. Kavousi-Fard, and W. Su. Optimal routing and charging of an electric vehicle fleet for high-efficiency dynamic transit systems. *IEEE Transactions on Smart Grid*, 9(4):3563–3572, 2016.

- [9] A. J. Conejo and L. Baringo. *Power system operations*. Springer, 2018.
- [10] A. Costa and A. S. Costa. Energy and ancillary service dispatch through dynamic optimal power flow. *Electric Power Systems Research*, 77(8):1047 – 1055, 2007.
- [11] S. Gopinath, H. Hijazi, T. Weisser, H. Nagarajan, M. Yetkin, K. Sundar, and R. Bent. Proving global optimality of acopf solutions. *Electric Power Systems Research*, 189:106688, 2020.
- [12] L. Gurobi Optimization. Gurobi optimizer reference manual, 2020.
- [13] Haiyan Chen, Jinfu Chen, and Xianzhong Duan. Multi-stage dynamic optimal power flow in wind power integrated system. In *2005 IEEE/PES Transmission Distribution Conference Exposition: Asia and Pacific*, pages 1–5, Aug 2005.
- [14] R. A. Jabr, S. Karaki, and J. A. Korbane. Robust multi-period opf with storage and renewables. *IEEE Transactions on Power Systems*, 30(5):2790–2799, Sep. 2015.
- [15] A. J. Lamadrid and T. Mount. Ancillary services in systems with high penetrations of renewable energy sources, the case of ramping. *Energy Economics*, 34(6):1959 – 1971, 2012.
- [16] Y. Levron, J. M. Guerrero, and Y. Beck. Optimal power flow in microgrids with energy storage. *IEEE Transactions on Power Systems*, 28(3):3226–3234, Aug 2013.
- [17] Y. Lin, K. Zhang, Z.-J. M. Shen, B. Ye, and L. Miao. Multistage large-scale charging station planning for electric buses considering transportation network and power grid. *Transportation Research Part C: Emerging Technologies*, 107:423 – 443, 2019.
- [18] A. Lorca and X. A. Sun. The adaptive robust multi-period alternating current optimal power flow problem. *IEEE Transactions on Power Systems*, 33(2):1993–2003, March 2018.
- [19] M. M. Moarefdoost, A. J. Lamadrid, and L. F. Zuluaga. A robust model for the ramp-constrained economic dispatch problem with uncertain renewable energy. *Energy Economics*, 56:310 – 325, 2016.
- [20] J. M. Morales, A. J. Conejo, H. Madsen, P. Pinson, and M. Zugno. *Integrating renewables in electricity markets: operational problems*, volume 205. Springer Science & Business Media, 2013.
- [21] S. Pfenninger and I. Staffell. Long-term patterns of european pv output using 30 years of validated hourly reanalysis and satellite data. *Energy*, 114:1251 – 1265, 2016.
- [22] Y. Riffonneau, S. Bacha, F. Barruel, and S. Ploix. Optimal power flow management for grid connected pv systems with batteries. *IEEE Transactions on Sustainable Energy*, 2(3):309–320, July 2011.
- [23] I. Staffell and S. Pfenninger. Using bias-corrected reanalysis to simulate current and future wind power output. *Energy*, 114:1224 – 1239, 2016.
- [24] Tong Wu, M. Rothleder, Z. Alaywan, and A. D. Papalexopoulos. Pricing energy and ancillary services in integrated market systems by an optimal power flow. *IEEE Transactions on Power Systems*, 19(1):339–347, 2004.
- [25] W. Wei, S. Mei, L. Wu, M. Shahidehpour, and Y. Fang. Optimal traffic-power flow in urban electrified transportation networks. *IEEE Transactions on Smart Grid*, 8(1):84–95, Jan 2017.
- [26] M. Xylia, S. Leduc, P. Patrizio, F. Kraxner, and S. Silveira. Locating charging infrastructure for electric buses in stockholm. *Transportation Research Part C: Emerging Technologies*, 78:183 – 200, 2017.
- [27] M. Xylia, S. Leduc, P. Patrizio, S. Silveira, and F. Kraxner. Developing a dynamic optimization model for electric bus charging infrastructure. *Transportation Research Procedia*, 27:776 – 783, 2017. 20th EURO Working Group on Transportation Meeting, EWGT 2017, 4-6 September 2017, Budapest, Hungary.

- [28] M. Yao, D. Molzahn, and J. L. Mathieu. An optimal power flow approach to improve power system voltage stability using demand response. *IEEE Transactions on Control of Network Systems*, pages 1–1, 2019.
- [29] M. Yetkin, B. R. Augustino, L. V. Synder, and A. J. Lamadrid. Co-optimizing the smart grid and electric public transit system. In *Proceedings of the TSL Second Triennial Conference*. INFORMS, 2020. Obtained from: <https://www.informs.org/Publications/Proceedings-of-the-TSL-Second-Triennial-Conference>.
- [30] Z. Yi, J. Smart, and M. Shirk. Energy impact evaluation for eco-routing and charging of autonomous electric vehicle fleet: Ambient temperature consideration. *Transportation Research Part C: Emerging Technologies*, 89:344 – 363, 2018.
- [31] A. Zakariazadeh, S. Jadid, and P. Siano. Multi-objective scheduling of electric vehicles in smart distribution system. *Energy Conversion and Management*, 79:43 – 53, 2014.
- [32] Zhongwei Wang, Jin Zhong, Dong Chen, Yuefeng Lu, and Kun Men. A multi-period optimal power flow model including battery energy storage. In *2013 IEEE Power Energy Society General Meeting*, pages 1–5, July 2013.
- [33] R. D. Zimmerman, C. E. Murillo-Sánchez, and R. J. Thomas. Matpower: Steady-state operations, planning, and analysis tools for power systems research and education. *IEEE Transactions on Power Systems*, 26(1):12–19, Feb 2011.

## Appendix A Nomenclature

<b>Sets</b>	
$\mathcal{N}$	set of nodes in the power network
$\mathcal{N}_g \subseteq \mathcal{N}$	set of nodes with conventional generators in the power network
$\mathcal{N}_r \subseteq \mathcal{N}$	set of nodes with renewable generators in the power network
$\mathcal{N}_b \subseteq \mathcal{N}$	set of candidate points for transit bus connection coupling the two systems
$\mathcal{L}$	set of lines present in the power network
$\mathcal{B}$	set of transit buses
$\mathcal{T}$	set of time periods
$\mathcal{T}_b$	set of off-schedule time periods for bus $b \in \mathcal{B}$
$\Omega$	set of scenarios for uncertain renewable generation
<b>Indices</b>	
$T_b^1, T_b^2$	first and last time periods in off-schedule of bus $b \in \mathcal{B}$ , respectively
<b>Parameters</b>	
$c^g$	conventional generation cost coefficients (linear)
$c'^g$	conventional generation cost coefficients (quadratic)
$c$	charging/discharging costs of transit buses
$c^+$	additional charging/discharging costs of transit buses
$c^r$	renewable generation cost coefficients
$c^{\text{shed}}$	costs of load-shedding in the power network
$c^{g,+}$	ramp-up costs of conventional generators
$c^{g,-}$	ramp-down costs of conventional generators
$p^d$	external demands present in the power grid
$\bar{\theta}$	limit on the voltage angles in the power network
$x$	reactance values of lines in the power network
$\bar{S}$	flow limits on lines in the power network
$\bar{p}^g$	conventional generation limits
$p^{\delta g}$	ramping limits of conventional generators
$e^1$	initial battery levels of transit buses (at the beginning of their off-schedules)

$\underline{e}$	lower limits on battery levels of transit buses
$\bar{e}$	upper limits on battery levels of transit buses
$s$	traversal energy consumption of transit buses over one time period
$\bar{p}^c$	limits on charging amounts of transit buses
$\bar{p}^{dc}$	limits on discharging amounts of transit buses
$\eta$	efficiency values of transit bus batteries
$\delta t$	duration of time in a single period
$\Delta t(\cdot, \cdot)$	required number of time steps to relocate between two charging stations
$\alpha$	convex combination coefficient
$\pi$	probabilities of scenarios
<b>Variables</b>	
$p^g$	conventional generation amounts
$p^r$	renewable generation amounts
$p^{d,shed}$	amounts of load-shedding
$p^{g,+}$	ramp-up amounts of conventional generators
$p^{g,-}$	ramp-down amounts of conventional generators
$p^c$	charging amounts of transit buses
$p^{dc}$	discharging amounts of transit buses
$p^{c,+}$	additional charging amounts of transit buses
$p^{dc,+}$	additional discharging amounts of transit buses
$p$	power flows on lines in the power network
$\theta$	voltage angles on nodes in the power network
$e$	battery levels of transit buses
$z$	assignment variables of transit buses to charging locations
$y$	indicator variables on the traversal status of transit buses

## Appendix B Complete formulation of the deterministic model

This MIQP formulation is given by:

$$\min (1 - \alpha) \sum_{t \in \mathcal{T}} \sum_{i \in \mathcal{N}_g} c_{it}^g p_{it}^g + c_{it}^{\prime g} (p_{it}^g)^2 + \alpha \sum_{t \in \mathcal{T}} \sum_{b \in \mathcal{B}} \sum_{i \in \mathcal{N}_b} c_{it} (p_{ibt}^c - p_{ibt}^{dc}) \quad (38)$$

subject to:

$$p_{it}^g - \sum_{b \in \mathcal{B}} p_{ibt}^c + \sum_{b \in \mathcal{B}} p_{ibt}^{dc} - p_{it}^d = \sum_{j: (i,j) \in \mathcal{L}} p_{ijt} - \sum_{j: (j,i) \in \mathcal{L}} p_{jit} \quad \forall i \in \mathcal{N}, t \in \mathcal{T} \quad (39)$$

$$p_{it}^g = 0 \quad \forall i \in \mathcal{N} \setminus \mathcal{N}_g, t \in \mathcal{T} \quad (40)$$

$$-\bar{\theta} \leq \theta_{it} \leq \bar{\theta} \quad \forall i \in \mathcal{N}, t \in \mathcal{T} \quad (41)$$

$$\theta_{1t} = 0 \quad \forall t \in \mathcal{T} \quad (42)$$

$$p_{ijt} = \frac{\theta_{it} - \theta_{jt}}{x_{ij}} \quad \forall (i, j) \in \mathcal{L}, t \in \mathcal{T} \quad (43)$$

$$-\bar{S}_{ij} \leq p_{ijt} \leq \bar{S}_{ij} \quad \forall (i, j) \in \mathcal{L}, t \in \mathcal{T} \quad (44)$$

$$0 \leq p_{it}^g \leq \bar{p}_{it}^g \quad \forall i \in \mathcal{N}_g, t \in \mathcal{T} \quad (45)$$

$$-p_{it}^{\delta g} \leq p_{i,t+1}^g - p_{it}^g \leq p_{it}^{\delta g} \quad \forall i \in \mathcal{N}_g, t \in \mathcal{T} \setminus \{T\} \quad (46)$$

$$e_{bT_b^1} = e_b^1 \quad \forall b \in \mathcal{B} \quad (47)$$

$$e_{bT_b^2} + \eta_b \sum_{i \in \mathcal{N}_b} p_{ibt}^c \delta t - \frac{1}{\eta_b} \sum_{i \in \mathcal{N}_b} p_{ibt}^{dc} \delta t - s_b y_{bT_b^2} = \bar{e}_b \quad \forall b \in \mathcal{B} \quad (48)$$

$$e_{b,t+1} = e_{bt} + \eta_b \sum_{i \in \mathcal{N}_b} p_{ibt}^c \delta t - \frac{1}{\eta_b} \sum_{i \in \mathcal{N}_b} p_{ibt}^{dc} \delta t - s_b y_{bt} \quad \forall b \in \mathcal{B}, t, t+1 \in \mathcal{T}_b \quad (49)$$

$$e_b \leq e_{bt} \leq \bar{e}_b \quad \forall b \in \mathcal{B}, t \in \mathcal{T}_b \quad (50)$$

$$0 \leq p_{ibt}^c \leq \bar{p}_b^c z_{ibt} \quad \forall i \in \mathcal{N}_b, b \in \mathcal{B}, t \in \mathcal{T} \quad (51)$$

$$0 \leq p_{ibt}^{dc} \leq \bar{p}_b^{dc} z_{ibt} \quad \forall i \in \mathcal{N}_b, b \in \mathcal{B}, t \in \mathcal{T} \quad (52)$$

$$p_{ibt}^c = 0, p_{ibt}^{dc} = 0 \quad \forall i \in \mathcal{N} \setminus \mathcal{N}_b, b \in \mathcal{B}, t \in \mathcal{T} \quad (53)$$

$$\sum_{i \in \mathcal{N}_b} z_{ibt} + y_{bt} = 1 \quad \forall b \in \mathcal{B}, t \in \mathcal{T}_b \quad (54)$$

$$z_{ibt} + z_{jbt'} \leq 1 \quad \forall t' \in \mathcal{T}_b, t < t' \leq t + \Delta t(i, j), \quad (55)$$

$$\forall i, j \in \mathcal{N}_b, i \neq j, b \in \mathcal{B}, t \in \mathcal{T}_b$$

$$z_{dbT_b^1} = 1 \quad d = \mathcal{N}_b(1), \forall b \in \mathcal{B} \quad (56)$$

$$y_{bt} = 0 \quad \forall b \in \mathcal{B}, t \in \mathcal{T} \setminus \mathcal{T}_b \quad (57)$$

$$z_{ibt} = 0 \quad \forall i \in \mathcal{N}_b, b \in \mathcal{B}, t \in \mathcal{T} \setminus \mathcal{T}_b \quad (58)$$

$$y_{bt} \in \{0, 1\} \quad \forall b \in \mathcal{B}, t \in \mathcal{T} \quad (59)$$

$$z_{ibt} \in \{0, 1\} \quad \forall i \in \mathcal{N}_b, b \in \mathcal{B}, t \in \mathcal{T} \quad (60)$$

Our objective (38) is to minimize a convex combination, with coefficient  $\alpha$ , of the total power generation cost and the charging/discharging cost of the transit buses. For each time period  $t \in \mathcal{T}$ , both the charging and discharging costs are given by  $c_{it}$ . These values, also known as locational marginal prices [15], represent the optimal dual values associated with the nodal balance equations of the power network. Hence, in the case of simultaneous charging and discharging, the costs and revenues will cancel each other out; that is, it is never (strictly) optimal to charge and discharge simultaneously. This simplifies the formulation since otherwise, one would need an extra set of binary variables indicating whether each vehicle is charging or discharging.

Constraints (39)-(45) are standard DC optimal power flow constraints except constraint set (39) additionally incorporates terms for charging and discharging in the nodal balance equations. Inequality (46) ensures that the ramping amount of generators is within the limit. Constraint sets (47) and (48) provide initial and final conditions on the battery levels of the transit buses respectively. Constraints (49) are battery level updates for the transit fleet, where the bounds on the battery levels are employed in (50). Constraints (51),(52) ensure that a battery can only charge/discharge if the transit bus is connected to a node in the power network.

Constraints (54) are assignment constraints specifying that a transit bus can either be connected to one of the possible nodes in the power network or relocating within the network. Then, constraint set (55) guarantees any relocation made throughout the horizon is feasible while ensuring that a transit bus cannot relocate in fewer time steps than the required travel time  $\Delta t(\cdot, \cdot)$ . Finally, equation (56) is the initial assignment of the transit buses to the depot node, whereas (57) and (58) ensure that assignment only occurs within the off-schedule periods of the vehicles. Note that the time periods in the formulation are inherently cyclic in their nature (i.e. considering hourly intervals, period 23 connects to period 0).

As a note related to the assumption on the capacities of charging stations, considering constant charging capacities per station  $C_i$ , depending on the specific application, one can incorporate the following constraint set:

$$\sum_{b \in \mathcal{B}} z_{ibt} \leq C_i \quad \forall i \in \mathcal{N}_b, t \in \mathcal{T} \quad (61)$$

## Appendix C Complete formulation of the two-stage stochastic formulation with recourse action as ramping up/down conventional generators

Now, we present the complete formulation:

$$\begin{aligned} \min \quad & (1 - \alpha) \left[ \sum_{t \in \mathcal{T}} \sum_{i \in \mathcal{N}_g} c_{it}^g p_{it}^g + c_{it}^{\prime g} (p_{it}^g)^2 + \sum_{\omega \in \Omega} \pi_\omega \left( \sum_{t \in \mathcal{T}} \sum_{i \in \mathcal{N}_r} c_{it}^r p_{it\omega}^r + \sum_{t \in \mathcal{T}} \sum_{i \in \mathcal{N}} c_{it}^{\text{shed}} p_{it\omega}^{d,\text{shed}} \right) \right] \\ & + (1 - \alpha) \sum_{\omega \in \Omega} \pi_\omega \sum_{t \in \mathcal{T}} \sum_{i \in \mathcal{N}_g} (c_{it}^{g,+} p_{it\omega}^{g,+} - c_{it}^{g,-} p_{it\omega}^{g,-}) + \alpha \sum_{t \in \mathcal{T}} \sum_{b \in \mathcal{B}} \sum_{i \in \mathcal{N}_b} c_{it} (p_{ibt}^c - p_{ibt}^{dc}) \end{aligned} \quad (62)$$

subject to:

$$p_{it}^g + p_{it}^r - \sum_{b \in \mathcal{B}} p_{ibt}^c + \sum_{b \in \mathcal{B}} p_{ibt}^{dc} - p_{it}^d = \sum_{j:(i,j) \in \mathcal{L}} p_{ijt} - \sum_{j:(j,i) \in \mathcal{L}} p_{jit} \quad \forall i \in \mathcal{N}, t \in \mathcal{T} \quad (63)$$

$$p_{it\omega}^r - p_{it}^r + p_{it\omega}^{g,+} - p_{it\omega}^{g,-} + p_{it\omega}^{d,\text{shed}} = \sum_{j:(i,j) \in \mathcal{L}} (p_{ijt\omega} - p_{ijt}) - \sum_{j:(j,i) \in \mathcal{L}} (p_{jit\omega} - p_{jit}) \quad \forall i \in \mathcal{N}, t \in \mathcal{T}, \omega \in \Omega \quad (64)$$

$$p_{it}^g = 0 \quad \forall i \in \mathcal{N} \setminus \mathcal{N}_g, t \in \mathcal{T} \quad (65)$$

$$p_{it}^r = 0 \quad \forall i \in \mathcal{N} \setminus \mathcal{N}_r, t \in \mathcal{T} \quad (66)$$

$$p_{it\omega}^r = 0 \quad \forall i \in \mathcal{N} \setminus \mathcal{N}_r, t \in \mathcal{T}, \omega \in \Omega \quad (67)$$

$$-\bar{\theta} \leq \theta_{it} \leq \bar{\theta} \quad \forall i \in \mathcal{N}, t \in \mathcal{T} \quad (68)$$

$$-\bar{\theta} \leq \theta_{it\omega} \leq \bar{\theta} \quad \forall i \in \mathcal{N}, t \in \mathcal{T}, \omega \in \Omega \quad (69)$$

$$\theta_{1t} = 0 \quad \forall t \in \mathcal{T} \quad (70)$$

$$\theta_{1t\omega} = 0 \quad \forall t \in \mathcal{T}, \omega \in \Omega \quad (71)$$

$$p_{ijt} = \frac{\theta_{it} - \theta_{jt}}{x_{ij}} \quad \forall (i, j) \in \mathcal{L}, t \in \mathcal{T} \quad (72)$$

$$p_{ijt\omega} = \frac{\theta_{it\omega} - \theta_{jt\omega}}{x_{ij}} \quad \forall (i, j) \in \mathcal{L}, t \in \mathcal{T}, \omega \in \Omega \quad (73)$$

$$-\bar{S}_{ij} \leq p_{ijt} \leq \bar{S}_{ij} \quad \forall (i, j) \in \mathcal{L}, t \in \mathcal{T} \quad (74)$$

$$-\bar{S}_{ij} \leq p_{ijt\omega} \leq \bar{S}_{ij} \quad \forall (i, j) \in \mathcal{L}, t \in \mathcal{T}, \omega \in \Omega \quad (75)$$

$$0 \leq p_{it}^g + p_{it}^{g,+} \leq \bar{p}_{it}^g \quad \forall i \in \mathcal{N}_g, t \in \mathcal{T} \quad (76)$$

$$p_{it}^{g,-} \leq p_{it}^g \quad \forall i \in \mathcal{N}_g, t \in \mathcal{T} \quad (77)$$

$$p_{it\omega}^{g,+} \leq p_{it}^{g,+} \quad \forall i \in \mathcal{N}_g, t \in \mathcal{T}, \omega \in \Omega \quad (78)$$

$$p_{it\omega}^{g,-} \leq p_{it}^{g,-} \quad \forall i \in \mathcal{N}_g, t \in \mathcal{T}, \omega \in \Omega \quad (79)$$

$$-p_{it}^{\delta g} \leq p_{i,t+1}^g - p_{it}^g \leq p_{it}^{\delta g} \quad \forall i \in \mathcal{N}_g, t \in \mathcal{T} \setminus \{T\} \quad (80)$$

$$0 \leq p_{it}^r \leq \bar{p}_{it}^r \quad \forall i \in \mathcal{N}_r, t \in \mathcal{T} \quad (81)$$

$$0 \leq p_{it\omega}^r \leq \bar{p}_{it\omega}^r \quad \forall i \in \mathcal{N}_r, t \in \mathcal{T}, \omega \in \Omega \quad (82)$$

$$0 \leq p_{it\omega}^{d,\text{shed}} \leq p_{it}^d \quad \forall i \in \mathcal{N}, t \in \mathcal{T}, \omega \in \Omega \quad (83)$$

$$0 \leq p_{it}^{g,+} \leq \bar{p}_{it}^{g,+} \quad \forall i \in \mathcal{N}_g, t \in \mathcal{T} \quad (84)$$

$$0 \leq p_{it}^{g,-} \leq \bar{p}_{it}^{g,-} \quad \forall i \in \mathcal{N}_g, t \in \mathcal{T} \quad (85)$$

$$p_{it\omega}^{g,+} \geq 0, p_{it\omega}^{g,-} \geq 0 \quad \forall i \in \mathcal{N}_g, t \in \mathcal{T}, \omega \in \Omega \quad (86)$$

$$e_{bT_b^1} = e_b^1 \quad \forall b \in \mathcal{B} \quad (87)$$

$$e_{bT_b^2} + \eta_b \sum_{i \in \mathcal{N}_b} p_{ibT_b^2}^c \delta t - \frac{1}{\eta_b} \sum_{i \in \mathcal{N}_b} p_{ibT_b^2}^{dc} \delta t - s_b y_{bT_b^2} = \bar{e}_b \quad \forall b \in \mathcal{B} \quad (88)$$

$$e_{b,t+1} = e_{bt} + \eta_b \sum_{i \in \mathcal{N}_b} p_{ibt}^c \delta t - \frac{1}{\eta_b} \sum_{i \in \mathcal{N}_b} p_{ibt}^{dc} \delta t - s_b y_{bt} \quad \forall b \in \mathcal{B}, t, t+1 \in \mathcal{T}_b \quad (89)$$

$$e_b \leq e_{bt} \leq \bar{e}_b \quad \forall b \in \mathcal{B}, t \in \mathcal{T}_b \quad (90)$$

$$0 \leq p_{ibt}^c \leq \bar{p}_b^c z_{ibt} \quad \forall i \in \mathcal{N}_b, b \in \mathcal{B}, t \in \mathcal{T} \quad (91)$$

$$0 \leq p_{ibt}^{dc} \leq \bar{p}_b^{dc} z_{ibt} \quad \forall i \in \mathcal{N}_b, b \in \mathcal{B}, t \in \mathcal{T} \quad (92)$$

$$p_{ibt}^c = 0, p_{ibt}^{dc} = 0 \quad \forall i \in \mathcal{N} \setminus \mathcal{N}_b, b \in \mathcal{B}, t \in \mathcal{T} \quad (93)$$

$$\sum_{i \in \mathcal{N}_b} z_{ibt} + y_{bt} = 1 \quad \forall b \in \mathcal{B}, t \in \mathcal{T}_b \quad (94)$$

$$z_{ibt} + z_{jbt'} \leq 1 \quad \forall t' \in \mathcal{T}_b, t < t' \leq t + \Delta t(i, j), \quad (95)$$

$$\forall i, j \in \mathcal{N}_b, i \neq j, b \in \mathcal{B}, t \in \mathcal{T}_b$$

$$z_{dbT_b^1} = 1 \quad d = \mathcal{N}_b(1), \forall b \in \mathcal{B} \quad (96)$$

$$y_{bt} = 0 \quad \forall b \in \mathcal{B}, t \in \mathcal{T} \setminus \mathcal{T}_b \quad (97)$$

$$z_{ibt} = 0 \quad \forall i \in \mathcal{N}_b, b \in \mathcal{B}, t \in \mathcal{T} \setminus \mathcal{T}_b \quad (98)$$

$$y_{bt} \in \{0, 1\} \quad \forall b \in \mathcal{B}, t \in \mathcal{T} \quad (99)$$

$$z_{ibt} \in \{0, 1\} \quad \forall i \in \mathcal{N}_b, b \in \mathcal{B}, t \in \mathcal{T} \quad (100)$$

Here, the objective function (62) is the summation of first-stage costs (which has already been captured by the deterministic objective function (38)) and second-stage costs including the expected renewable generation costs and expected ramping costs. In addition to the constraints captured in the deterministic model in Section 3 are the second-stage nodal balance (64) and flows (69), (71), (73), (75); limits on renewable generation (81), (82); limits on second-stage ramping (76), (78), (79); and limits on shedding in the second stage (83). The main differences from the two-stage stochastic OPF formulation presented in [20] are constraints on the transit bus battery levels (87)-(90), charging limits (91)-(93), and transportation constraints (94)-(100). More importantly, we have each of the OPF constraints repeated for multiple time periods rather than a single time period presented in [20]. The inclusion of multiple periods, and their coupling by the presence of batteries, increase the complexity of the problem dramatically.

Note that we have two sets of ramping quantities  $p_{it}^{\delta g}$ , and variables  $(p_{it}^{g,+}, p_{it}^{g,-})$  associated with ramping in different time periods. Specifically, the parameters  $p_{it}^{\delta g}$  serve as upper bounds on the ramping of conventional generators between two time periods in the formulation, whereas the variables  $(p_{it}^{g,+}, p_{it}^{g,-})$  correspond to ramping of conventional generators between the two stages of the stochastic formulation.

## Appendix D Two-stage stochastic multi-period OPF formulation to obtain prices of charging/discharging

In this section, we present a baseline OPF formulation in order to estimate the first-stage and second-stage prices of charging/discharging in formulations presented in Sections 4.2 and 4.1. The complete formulation is as follows:

$$\begin{aligned} \min \quad & \sum_{t \in \mathcal{T}} \sum_{i \in \mathcal{N}_g} c_{it}^g p_{it}^g + c_{it}^{lg} (p_{it}^g)^2 + \sum_{\omega \in \Omega} \pi_\omega \left( \sum_{t \in \mathcal{T}} \sum_{i \in \mathcal{N}_r} c_{it}^r p_{it\omega}^r + \sum_{t \in \mathcal{T}} \sum_{i \in \mathcal{N}} c_{it}^{\text{shed}} p_{it\omega}^{d,\text{shed}} \right) \\ & + \sum_{\omega \in \Omega} \pi_\omega \sum_{t \in \mathcal{T}} \sum_{i \in \mathcal{N}_g} (c_{it}^{g,+} p_{it\omega}^{g,+} - c_{it}^{g,-} p_{it\omega}^{g,-}) \end{aligned} \quad (101)$$

subject to:

$$(c_{it}) : p_{it}^g + p_{it}^r - p_{it}^d = \sum_{j:(i,j) \in \mathcal{L}} p_{ijt} - \sum_{j:(j,i) \in \mathcal{L}} p_{jit} \quad \forall i \in \mathcal{N}, t \in \mathcal{T} \quad (102)$$

$$(c_{it\omega}) : p_{it\omega}^r - p_{it}^r + p_{it\omega}^{g,+} - p_{it\omega}^{g,-} + p_{it\omega}^{d,\text{shed}} = \sum_{j:(i,j) \in \mathcal{L}} (p_{ijt\omega} - p_{ijt}) - \sum_{j:(j,i) \in \mathcal{L}} (p_{jit\omega} - p_{jit})$$

$$\forall i \in \mathcal{N}, t \in \mathcal{T}, \omega \in \Omega \quad (103)$$

$$p_{it}^g = 0 \quad \forall i \in \mathcal{N} \setminus \mathcal{N}_g, t \in \mathcal{T} \quad (104)$$

$$p_{it}^r = 0 \quad \forall i \in \mathcal{N} \setminus \mathcal{N}_r, t \in \mathcal{T} \quad (105)$$

$$p_{it\omega}^r = 0 \quad \forall i \in \mathcal{N} \setminus \mathcal{N}_r, t \in \mathcal{T}, \omega \in \Omega \quad (106)$$

$$-\bar{\theta} \leq \theta_{it} \leq \bar{\theta} \quad \forall i \in \mathcal{N}, t \in \mathcal{T} \quad (107)$$

$$-\bar{\theta} \leq \theta_{it\omega} \leq \bar{\theta} \quad \forall i \in \mathcal{N}, t \in \mathcal{T}, \omega \in \Omega \quad (108)$$

$$\theta_{1t} = 0 \quad \forall t \in \mathcal{T} \quad (109)$$

$$\theta_{1t\omega} = 0 \quad \forall t \in \mathcal{T}, \omega \in \Omega \quad (110)$$

$$p_{ijt} = \frac{\theta_{it} - \theta_{jt}}{x_{ij}} \quad \forall (i, j) \in \mathcal{L}, t \in \mathcal{T} \quad (111)$$

$$p_{ijt\omega} = \frac{\theta_{it\omega} - \theta_{jt\omega}}{x_{ij}} \quad \forall (i, j) \in \mathcal{L}, t \in \mathcal{T}, \omega \in \Omega \quad (112)$$

$$-\bar{S}_{ij} \leq p_{ijt} \leq \bar{S}_{ij} \quad \forall (i, j) \in \mathcal{L}, t \in \mathcal{T} \quad (113)$$

$$-\bar{S}_{ij} \leq p_{ijt\omega} \leq \bar{S}_{ij} \quad \forall (i, j) \in \mathcal{L}, t \in \mathcal{T}, \omega \in \Omega \quad (114)$$

$$0 \leq p_{it}^g + p_{it}^{g,+} \leq \bar{p}_{it}^g \quad \forall i \in \mathcal{N}_g, t \in \mathcal{T} \quad (115)$$

$$p_{it}^{g,-} \leq p_{it}^g \quad \forall i \in \mathcal{N}_g, t \in \mathcal{T} \quad (116)$$

$$p_{it\omega}^{g,+} \leq p_{it}^{g,+} \quad \forall i \in \mathcal{N}_g, t \in \mathcal{T}, \omega \in \Omega \quad (117)$$

$$p_{it\omega}^{g,-} \leq p_{it}^{g,-} \quad \forall i \in \mathcal{N}_g, t \in \mathcal{T}, \omega \in \Omega \quad (118)$$

$$-p_{it}^{\delta g} \leq p_{i,t+1}^g - p_{it}^g \leq p_{it}^{\delta g} \quad \forall i \in \mathcal{N}_g, t \in \mathcal{T} \setminus \{T\} \quad (119)$$

$$0 \leq p_{it}^r \leq \bar{p}_{it}^r \quad \forall i \in \mathcal{N}_r, t \in \mathcal{T} \quad (120)$$

$$0 \leq p_{it\omega}^r \leq \bar{p}_{it\omega}^r \quad \forall i \in \mathcal{N}_r, t \in \mathcal{T}, \omega \in \Omega \quad (121)$$

$$0 \leq p_{it\omega}^{d,\text{shed}} \leq p_{it}^d \quad \forall i \in \mathcal{N}, t \in \mathcal{T}, \omega \in \Omega \quad (122)$$

$$0 \leq p_{it}^{g,+} \leq \bar{p}_{it}^{g,+} \quad \forall i \in \mathcal{N}_g, t \in \mathcal{T} \quad (123)$$

$$0 \leq p_{it}^{g,-} \leq \bar{p}_{it}^{g,-} \quad \forall i \in \mathcal{N}_g, t \in \mathcal{T} \quad (124)$$

$$p_{it\omega}^{g,+} \geq 0, p_{it\omega}^{g,-} \geq 0 \quad \forall i \in \mathcal{N}_g, t \in \mathcal{T}, \omega \in \Omega \quad (125)$$

This formulation is a direct extension of the two-stage single-period optimal power formulation presented by Morales et al. [20]. Specifically, we use the optimal dual variables  $c_{it}, c_{it\omega}^+$  associated with constraints (102) and (103), respectively, to determine the first-stage and second-stage charging/discharging prices.